The Hebrew University of Jerusalem – The Edmond &Lily Safra Center for Brain Sciences

Graduate thesis for a research M.Sc. in brain sciences

Single Neuron Functional Analysis – Information Theoretical Approach

Nitzan Luxembourg

Supervisor: Prof. Idan Segev

The Edmond and Lily Safra Center for Brain Sciences

25.2.2024

Contents

Abstract

This thesis investigates the functional roles of single neurons through an information theoretical approach, primarily focusing on the input-output (I/O) functional relations in various neuronal models. Emphasizing the concept of mutual information, the study explores how neuronal heterogeneity and complexity contribute to information processing capabilities at the single neuron level. By comparing detailed and reduced models of Rat Layer 5b pyramidal cells and Human Layer 2/3 pyramidal cells, this research provides insights into the computational power of individual neurons.

The analysis employs mutual information and entropy measures to quantify the amount of information transferred from presynaptic to postsynaptic neurons. It investigates how structural and biophysical properties, including dendritic morphology, synaptic input distribution, and ionic conductance variability, influence these measures.

Key findings include the observation that NMDA-based synapses enhance neuronal complexity, and that the increase in synaptic conductance can alter a neuron's computational properties. We hypothesis that neurons exhibit a spectrum of computational capabilities, with some neurons processing more information (high mutual information) and others maintaining stability in representations (low mutual information). These findings have implications for understanding the diversity of neuronal computation in health and disease and provide a foundation for future research in brain sciences and computational neuroscience.

Keywords: Single Neuron Computation, Entropy, Mutual Information ,Complexity.

Introduction

The brain's remarkable ability to process information relies heavily on the heterogeneity of its constituent neurons, previous studies, such as in Perez-Nieves et al. [1], who have demonstrated that heterogeneity in spiking neural networks enhances performance on various tasks, particularly those with rich intrinsic temporal structures. Given the importance of heterogeneity in both theory and biology, a deeper understanding of its functional role at the single neuron level is essential.

Studying the input-output functional relations of a variety of single neurons is crucial for several reasons. First, it provides insights into the basic building blocks of neural computation, allowing us to better understand how individual neurons process and transmit information [2]. This knowledge is fundamental for understanding neural computation in more complex neural circuits and systems, leading to better comprehension of higher brain functions.

Second, by associating physiological markers and characteristics with functional traits, we can define biophysical mechanisms that contribute to irregular neural computation. This understanding can aid researchers in pinpointing specific cellular targets for therapeutic interventions, thereby promoting the creation of targeted therapies to reinstate normal neuronal function in neurological disorders.

In this thesis, we aim to explore the input-output functional relations of multiple compartmental models of single neurons, focusing on how heterogeneity, in structure and in biophysical properties, contributes to neuronal dynamics and computations. Multiple compartmental models offer a biologically motivated approach with close correspondence to the underlying biophysical properties of neurons and their membrane ion channels [3]. By using these models, we can investigate the functional impact of diverse types of heterogeneity, such as morphological complexity, spatial distribution of synaptic inputs, and variability of ionic conductance, on the input-output relationship of single neurons.

Through this investigation, we hope to shed light on the complex interplay between various forms of neuronal heterogeneity and the input-output (I/O) functional relations of single neurons. Ultimately, this deeper understanding of neuronal heterogeneity and the I/O relations of single neurons may provide new insights into the brain's efficient and robust information processing capabilities, provide a foundation for future research on neural computation and function, and aid in the development of targeted interventions for neurological disorders.

Neuronal Variability and its Different Measures

The astounding variability observed in nature is a testament to the complexity of biological systems. This diversity is mirrored in the nervous system, where neurons exhibit a wide range of variability in aspects such as ion channel types, morphology, and other intrinsic properties. A key question in neuroscience is whether brain function stems solely from the connectivity between neurons or if it is also due to the inherent computational capabilities of individual neurons. In other words, are all neurons born equal, or do they possess distinct computational properties that contribute to the diversity of behaviors observed in nature?

Traditionally, the firing rate of neurons has been utilized as a metric to characterize the computational capabilities of various brain modules. This approach reflects the long-standing focus in neuroscience on how the frequency of neuronal firing correlates with different cognitive and functional processes within the brain. For instance, in the motor cortex, studies have shown that the firing rate is closely linked to limb movement, with neurons firing at different rates depending on the direction of an arm movement [4]. In the visual cortex, particularly in areas like V1, the firing rate of neurons is correlated with visual stimuli, such as orientations of lines or edges in the visual field [5]. In the hippocampus, which is crucial for memory formation and spatial navigation, 'place cells' have been shown to fire at higher rates when an animal is in or moving towards a specific location [6]. Similarly, in the auditory cortex, the firing rate of neurons can be linked to the processing of sound frequencies, with certain neurons firing at higher rates in response to specific frequencies [7].

However, relying on rate coding may not fully encapsulate the wide variability among neurons, as it falls short in explaining phenomena like sparse coding, millisecond-scale computation, and adaptation. Alternative measures, such as the Fano factor and coefficient of variance, offer more nuanced ways to quantify and understand neuronal diversity. [8] [9]

The Fano factor is a measure of the dispersion of probability distribution, specifically defined as the ratio of the variance to the mean of a neuron's spike count. A Fano factor greater than one indicates greater variability than expected for a Poisson process, while a value less than one suggests a more regular firing pattern.

The coefficient of variance, on the other hand, is the ratio of the standard deviation to the mean of the inter-spike interval (ISI) distribution. This measure can provide insights into the temporal structure of a neuron's firing pattern and its underlying computational properties.

By examining the Fano factor and coefficient of variance, we can delve deeper into the computational capabilities of individual neurons and determine whether these properties contribute to the observed variability in behaviors and coping mechanisms among species. However, these measures alone may not be sufficient to fully capture the intricacies of neuronal computation.

This is where mutual information comes into play. As a concept first introduced by Claude Shannon in his ground-breaking work on information theory [10], mutual information provides a quantitative framework for analyzing the relationship between input and output signals in complex systems, including the intricate computations performed by single neurons in the brain. We will show that by utilizing mutual information, we might gain a more comprehensive understanding of the input-output relationships and computational capabilities of individual neurons [3], thereby shedding light on the power of variability in nature.

The study of mutual information offers a promising avenue for investigating the computational properties of single neurons and their potential role in shaping the diverse behaviors observed in nature. By complementing traditional measures like firing rate, Fano factor, and coefficient of variance with mutual information analysis, we can deepen our understanding of the factors that contribute to the astonishing variability in biological systems.

Neurons as Complex Computational Devices

When the term "neuron" is used in machine learning research, it implies a perceptron as introduced by Rosenblatt [11]. However, biological neurons are quite distinct from their artificial counterparts. Indeed, Poirazi et al. demonstrated that a more accurate description of a single CA1 pyramidal neuron can be achieved using a 2-layer neural network [12]. Furthermore, Moldwin et al. showed that a biological neuron can emulate the perceptron, concluding that the computational power of a single perceptron is just a subset of the computational capabilities of a single biological neuron [13], e.g. neuron can solve the XOR problem which infeasible in single perceptron as presented by as shown by [14] .

Recently, Beniaguev et al. [15] have demonstrated that the presence or absence of NMDA receptors in the dendrites of cortical pyramidal neurons affects the “depth” of the analogous deep neural network (DNN) for this neuron. This implies that the presence of NMDA receptor

activation in dendrites might result in a more complex, layer-wise computation compared to AMPA receptor-based computation [15]. While various models exist that describe different morphologies, cable properties, and ion channels, our understanding of the computational power of individual neurons and the extent of variability in computational capabilities among different neurons remains limited.

Artificial Neural Network Complexity Comparison

Artificial Neural Networks (ANNs) have revolutionized computational neuroscience by providing a powerful tool for modeling biological neural systems. However, understanding and comparing the complexity of different models remains a challenging task. Complexity here not only refers to architectural intricacy but also to how effectively and efficiently the model can replicate real-world biological phenomena.

In this study, we direct our focus towards the Rat Layer 5b pyramidal cell [16], a subject of extensive research, and compare it to an analytical reduction by Amsalem et. al. [17]. This reduction simplifies the neuron by mapping active channels and synapses based on the electrotonic (cable) distance of the particular synapse and ion channel from the soma. Amsalem et al. have shown that this approach can replicate voltage dynamics and spike timing across various input regimes, forming a vital part of our analysis.

Our comparison consists of two parts: the ANN-based modeling of these structures, and a more detailed comparison of the Rat L5b pyramidal cell with its reduction, involving training the same instance of neural networks on different postsynaptic outputs (Figure 2).

One of the significant findings in Beniaguev et al. [15] is that the best-fitted model often correlates with the underlying complexity of the system. Simpler models that capture essential features of the system can often provide better fits to empirical data than more complex models loaded with redundant parameters. This phenomenon is particularly observed in our study, where the neural network with the reduction postsynaptic output fitted the data better than the original model.

By investigating these complexities and simplicities, we aim to shed light on the most efficient and accurate representation of the neural systems in question. The study's broader

objective is to contribute to the seamless convergence of artificial intelligence with biological neural functions, ensuring more precise modeling techniques in computational neuroscience.

We will delve into the methodologies used, the insights obtained, and how the rate of the model might affects the comparison, offering a comprehensive view that could pave the way for future research and applications in both computational modeling and biological understanding of neural systems.

Mutual Information and Complexity

In this investigation, we explored the role of neurons as communication channels and examined the intricate computations performed by individual neurons in the brain. By doing so, we aimed to determine the amount of information that transmitted from the presynaptic neuron to the postsynaptic neuron.

The human brain exhibits vast connectivity; for example, a single CA1 pyramidal cell possesses ~30,000 excitatory connections and ~1,700 inhibitory connections [18]. Despite this extensive connectivity, the neuron produces a single output. From a mathematical perspective, a single neuron can be viewed as a probabilistic function that maps a high-dimensional binary time series (input) to a single-dimensional binary time series (output). It is intriguing to explore the significance of individual synapses on the output, as demonstrated by previous research [3].

By employing mutual information, we can quantify the amount of information processed by a neuron from its presynaptic inputs. Furthermore, we can determine the strength of the connection between the presynaptic inputs and the postsynaptic outputs. The number of bits per milliseconds that are being transferred from the synapses to the axon implies the orchestrated power that the synapses have conveying information and the richness of patterns that they can hold.

Mutual information, therefore, serves as a powerful tool to investigate the information processing capabilities of single neurons and uncover the complexities inherent in neural communication.

Mutual Information Comparisons

The interpretation of the rate's influence on comparison could be ambiguous; is a three-spike burst less consistent than three separate spikes? Evidence has illustrated that a lone neuron can exhibit a spectrum of burst patterns, influenced by external disruptions caused by synapses and internal elements like channel noise. The introduction of minimal noise amplifies this variability, making the neuron highly responsive to random fluctuations and resulting in chaotic and irregular burst patterns, notably during transitions between distinct activity states. This highlights the intricate and adaptive characteristics of neuronal behavior, where slight variations can induce a range of unpredictable activity patterns [19].

One approach to measure these variations is information theory. This technique does not capture the entirety of computational complexity but focuses on assessing the volume of information traversing the communication channel represented by the individual neuron. It quantifies the average bits transferred from the presynaptic neurons to the neuron axon, offering insights into the informational exchange occurring within these neural networks.

We have the presynaptic input X the postsynaptic output Y and the neuron which act as a function $f: X \to Y$ then we want to examine the transfer of the message $X \to Y$. Focusing on the number of bits that pass between the input and output could indicate how selective the neuron is to certain $x \in X$ and this selectivity will be the mutual information, as this is higher this means that the postsynaptic neuron conveys high amount of information in his output on the activations of the presynaptic inputs. In our model we assume no intrinsic noise, therefore it is equivalent to calculating the postsynaptic neuron spike trains entropy (See Methods). A neuron with high sensitivity to all the synapses will result with high entropy and the constant neuron would have an entropy of zero. Choosing presynaptic inputs is a crucial step in the comparison process since one presynaptic input one neuron might be tuned to certain stimuli while others might not hold any information about the event that is being processed.

Pseudorandom Binary Sequences in the Neuronal Context

Pseudorandom binary sequences (PRBS) are deterministic sequences that appear random. They typically have balanced counts of ones and zeros, lack long runs of identical values, and possess constrained cross-correlations. Within the framework of a deterministic biophysical model of a neuron, the ideal scenario is for the neuron to attain maximum entropy. This is

achieved when the neuron's firing rate is at $\frac{T}{\Delta t} \cdot \frac{1}{2}$, indicating that it is responding to inputs and generating outputs at its peak efficiency. Additionally, the output should be as unpredictable as a pseudorandom binary sequence (PRBS), characterized by a normalized entropy of 1. Both these criteria collectively define the state of maximum entropy for the neuron. When a neuron's firing achieves this level of unpredictability, it essentially acts as a pseudorandom generator, producing outputs that seem random and are hard to predict from its inputs. Without understanding the neuron's inherent properties or the nature of its inputs, such behavior would indeed appear random.

The Unceasing Neuron: A Study of Zero Normalized Entropy

While in the first case we described a neuron that is the perfect storm in the other case a neuron that its normalized entropy is zero would imply that the number of bits that it needs to react are zero which might seems as the case of dead neuron , even though without knowing its nature we might never know if the neuron do responds to a signal and may need an infinite recording time that will display all the possible permutations in order to get the first irregular spike, thus the neuron can be viewed as highly selective to the pattern for which it reacts.

Navigating the Spectrum: From Perfect Noise to Inert Neuronal Response

The middle ground between these extremes represents a rich area of complexity, Calbet et. al. [20] defined statistical complexity, this measure attempts to capture the interplay between order and disorder in a system, being zero for both completely ordered (e.g., a crystal) and completely disordered (e.g., an ideal gas) systems. It achieves non-zero values for systems that are neither fully ordered nor fully disordered, reflecting a more "complex" behavior. Statistical complexity depends on the entropy and the disequilibrium, which measures the deviation from an equiprobable distribution of states.

Research by Fuentes et al. [18] demonstrates that true complexity is captured within normalized entropy values of 0.45-0.7, away from the boundaries. This region encapsulates the dynamic and nuanced nature of chaotic nonlinear dynamic (not exclusively), where neither perfect noise nor complete non-responsiveness dominates.

Furthermore, the landscape between these extremes can be challenging to navigate. Since the minimum and maximum boundaries are closer at the edges, differentiation between neuron

response and noise may be increasingly difficult. The sensitivity to changes in entropy near the boundaries might provide valuable insights into the neuron's adaptability and selectivity.
By investigating this spectrum, we gain a more profound understanding of the complex interplay between noise and order within the neuronal context. This exploration may open doors to new dimensions of research, including applications in understanding neurological disorders, enhancing artificial neural networks, or even unravelling the hidden complexities of cognitive processes. Through a combination of analytical and computational methods, this section attempts to bridge the gap between theory and practice, laying the groundwork for future investigations in computational neuroscience.

Shiner, Davison and Landsberg (SDL) Statistical Complexity Comparisons

The Shiner, Davison, and Landsberg (SDL) [21] statistical complexity measure provides another dimension to the analysis of neuronal behaviors. While entropy focuses on the unpredictability of a system, SDL statistical complexity considers both the structure and randomness within the data. It extends the concept of entropy by introducing a more comprehensive evaluation that captures not only the disorder but also the ordered patterns in the system. This measure allows us to better understand the underlying complexities in neuronal activity, beyond what is achievable by looking at entropy alone.

This complementary approach to mutual information and entropy provides a richer landscape for understanding the subtle intricacies of neural communication. In the subsequent sections, we will add to the comparison the SDL statistical complexity, aiming to draw insightful conclusions on the organization and complexity inherent in neuronal interactions.

Results

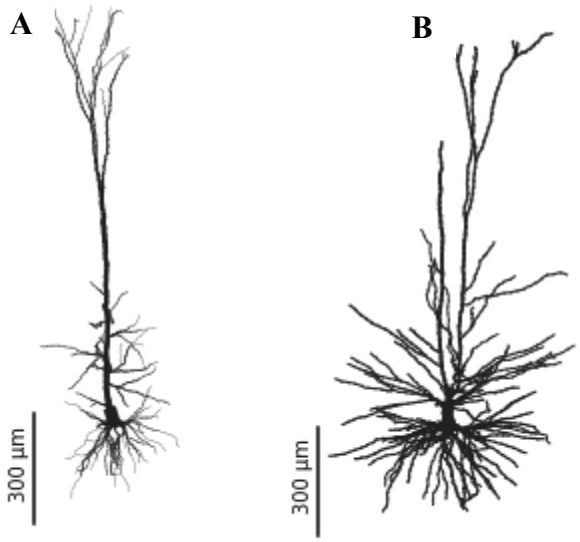

Figure 1. The Neuron Models morphologies. A. Rat layer 5 pyramidal cell model developed by Hay et. al. *[16]* B. Human layer 2/3 pyramidal cell model by Eyal et. al. *[22]*. These cells are examples of cell-models used in the present study.

Comparing the Complexity Measures to Detailed versus Reduced Models of L5b Pyramidal Cell using Analogous ANNs

In the first part of this study, we compared the I/O complexity of the detailed model [16] versus the reduced model [17] of L5b rat pyramidal neuron, using the corresponding ANNs for single neurons as discussed in Beniaguev et al. [15] . Our approach involved a slight adjustment in Beniaguev et al. methodology for a more tailored comparison. This entailed using an identical ANN for both models (the detailed and the reduced) to assess the learning difficulty (by the respective ANN) to replicate the I/O data obtained from each model. The process started with the stimulation of the detailed (Fig. 1B) and the reduced model (Fig. 1C) using the same random presynaptic input. We then trained two identical AANs on this input/output data, each aiming to learn (and closely replicate) the response of the respective neuron model. We then "deepened" the ANN (adding more layers to it) and repeated this comparison (Fig. 2). The effectiveness of learning was subsequently assessed using the Area Under the Curve (AUC) as a measure for the capability of the ANN to replicate the respective models (see Methods - Training and Comparing ANN).

In our investigation, we focused on the effects of model simplification on the learning efficiency of Artificial Neural Networks (ANNs). This was achieved by training two identical ANNs with the same presynaptic inputs but with outputs derived from two different models (Figure 2). One ANN was trained using the output from a simplified model, while the other utilized the output from the original, more complex model, as illustrated in Figure 2. Our findings shows that the ANN trained with the output from the simplified model demonstrated enhanced data fitting capabilities in comparison to the one trained with the output from the original model (Figure 3). This observation underscores the benefits of model simplification in improving the learning process of ANNs. The simplified model, with its reduced complexity and potentially fewer variables, was more effectively replicated by the ANN (compare blue to red lines in Figure 3).

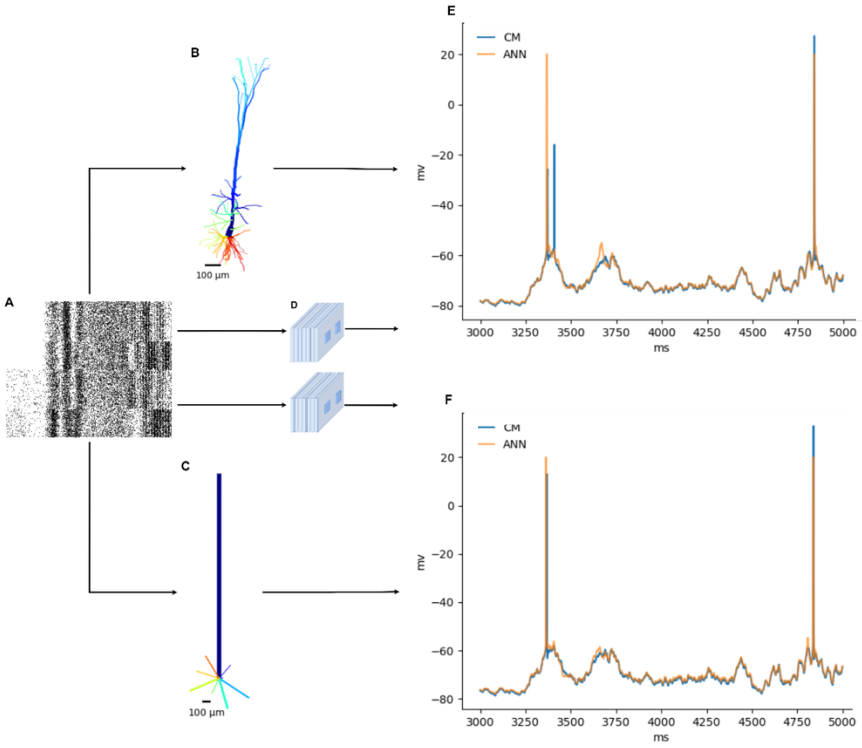

Figure 2. ANN based Model Comparison: **A.** Presynaptic input (raster plot) used to activate the detailed and the respective reduced model (in B, C). **B.** L5bPC detailed compartmental model. **C.** The reduced model of the cell shown in B as described by Amsalem et. al. *[17]*. **D.** Two identical ANN are trained on the same input data and the target was the output of B and C, respectively **E.** Evaluation of the ANN model (orange) where the ground truth is the output of model show in B (Blue). **F** Same as E, but here the ground truth is the output of the reduced model shown in C.

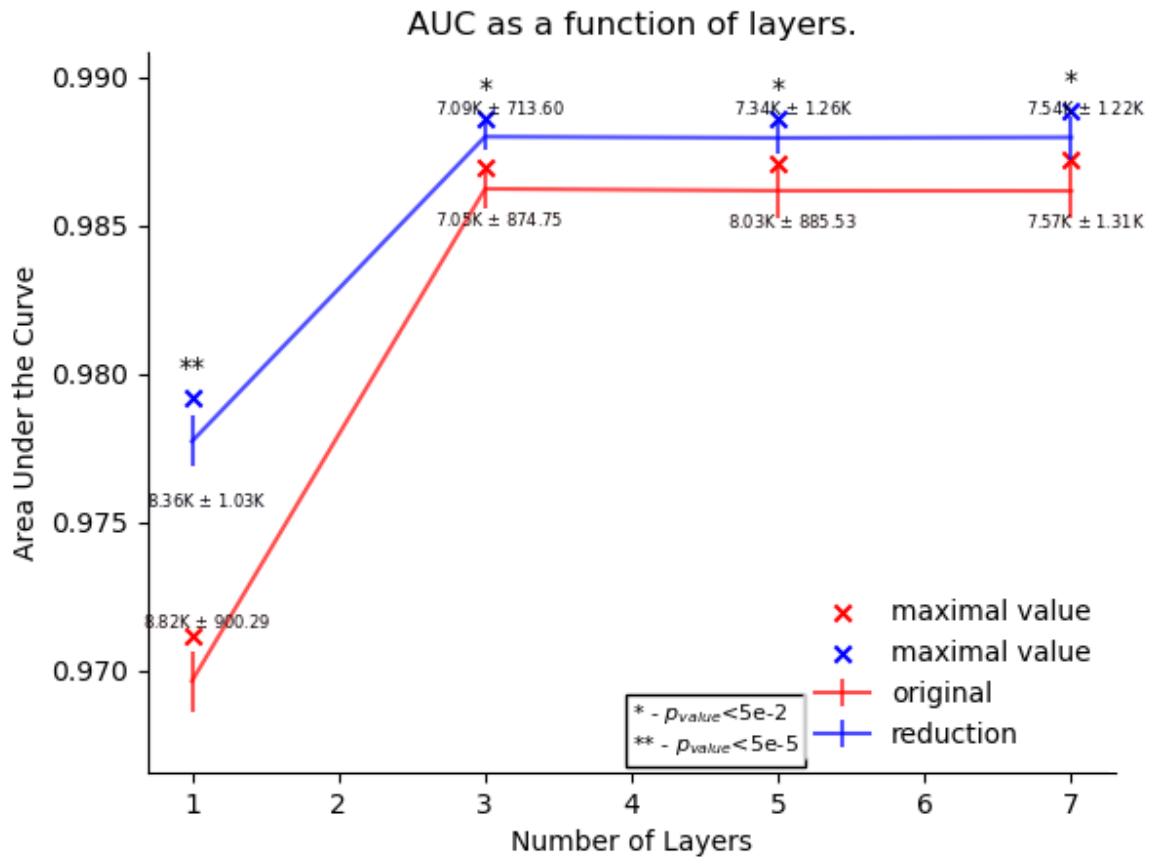

Figure 3. Comparative Analysis of ANN Learning Efficiency on Detailed versus Reduced L5b Neuron Models. AUC as a function of the number of layers in the analogue ANN for the detailed (red) and reduced (blue) models shown in Fig. 1B&C respectively. Each ANN was trained on postsynaptic outputs from two versions of the Rat L5b pyramidal cell model (the ground truth). The 'number of steps' displayed alongside each case corresponds to the training duration at which the network converged maximal score. The highest performing networks in each scenario are denoted with red and blue 'X' signs, corresponding to those trained on the original and reduced models, respectively. This distinction highlights the significant differences in AUC scores, underscoring the impact of model complexity on neural network training efficacy (n=4). Significance levels are indicated by * for p value <0.05 and ** for p value < 0.00005

In the analysis, we avoided subjective interpretation of the data, focusing instead on algorithmic convergence and accuracy measurements to ascertain the simplicity of the presynaptic input patterns in each model. Our findings were promising, yet they revealed a notable aspect: the success rates of the networks varied with the firing rate of the model. This

variation implies that the rate at which a model operates could significantly influence the outcome of such comparisons, indicating a need for careful consideration of model rates in future analyses.

The comparative analysis of the detailed and reduced models of L5b rat pyramidal neurons, conducted using artificial neural networks (ANNs), yields several pivotal insights. It firstly substantiates the hypothesis that simplifying a neuronal model can enhance the efficiency with which ANNs learn. This conclusion is drawn from the observation that the ANN, when trained with outputs from the simplified model, exhibited markedly superior data fitting capabilities compared to its performance with outputs from the more complex model.

This study is particularly significant as it suggests a potential correlation between the morphological complexity of neurons and their computational complexity. Employing identical ANNs to learn from both the detailed and reduced models underscores this hypothesis. Notably, the enhanced ability of the ANN to replicate the reduced model implies that morphological intricacies significantly contribute to neuronal computation, as compared to their reduced counterparts.

Furthermore, this research makes a substantial contribution to the field of computational neuroscience. It demonstrates how the simplification of models can be beneficial in the training of neural networks. The application of Area Under the Curve (AUC) as a metric for assessing the ANNs' ability to replicate the respective models introduces an objective dimension to this comparison, thereby advancing beyond the subjective interpretations of data previously outlined by Beniaguev et al. [15].

In conclusion, this study not only aligns with but also builds upon the work of Beniaguev et al. [15] and Amsalem et al. [17]. It offers a nuanced comparison between the original neuronal models and their reduced versions using ANNs, thereby enriching our understanding of the relationship between neuronal morphology and computational complexity.

Comparison of Model Complexity using Mutual Information

To deepen our understanding of neuronal model complexity, this section introduces two novel experiments employing mutual information as a measurement tool.

1. Resting Battery Modulation: The first experiment investigates the impact of altering the resting battery of the model on the statistics of the spiking output. In a leaky integrate-and-fire model with current injection and noise, the proximity of the resting battery to the threshold

influences the neuron's output irregularity. This is attributed to the neuron becoming more sensitive to noise and less to equilibrium forces as the resting potential approached the spike threshold. We believe that by making the model less active, it will produce outcomes similar to what we see with the leaky integrate-and-fire model.

2. Maximal Conductance Variation: The second experiment involves modifying the maximal synaptic conductances, effectively enhancing both excitatory and inhibitory forces and their (nonlinear) interplay. This manipulation is expected to alter the normalized entropy due to the disturbed balance between these forces. Particularly in non-linear synaptic ion channels (the NMDA-receptor)..

Model Variants for Examination: We will examine these alterations across four different models to assess their impact on complexity and information processing (as seen at Figure 1):

- Rat L5PC, as detailed in [16].
- Rat L5PC without NMDA channels, a variation of the first model.
- Human L23PC, as described in [22].
- A hybrid model combining the Human L23PC physiology with the Rat L5PC morphology.

These experiments aim to provide a comprehensive understanding of how variations in model parameters affect the complexity and information processing in neuronal models.

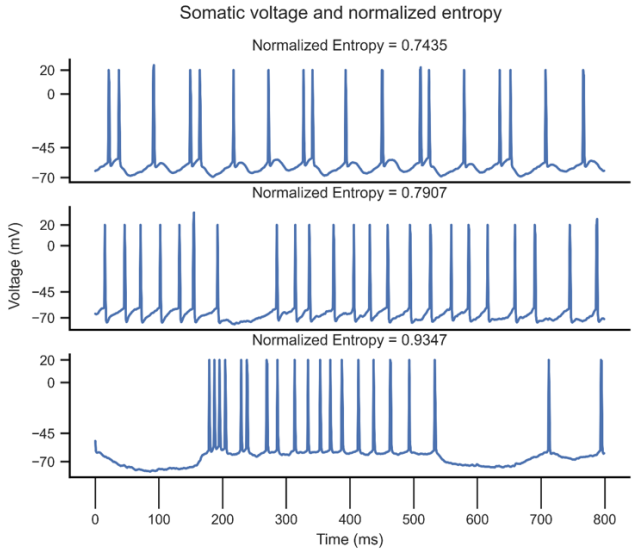

Figure 4. An Example of Different Traces with Varying Normalized Entropy Values, demonstrating the importance of normalized entropy in spike train analysis. Each trace represents somatic voltage responses over time, with the corresponding normalized entropy (at top). As the spike activity becomes less regular the normalized entropy increases.

Resting Battery Shift Models

In a basic experiment using mutual information to assess model complexity, we compare two versions of a Rat Layer 5b Pyramidal Cell model [16]: one with NMDA synapses and one without (Figure 5). Both models are subjected to the same inputs, but we adjust their resting potential differently. This adjustment leads to different levels of direct current (resting battery) shifts in the neurons' passive state(i.e., when active components of the model, such as voltage gated channels, are absent or inactive in the whole model). As a result, the average voltage across the neuron's soma changes, although the point at which the neuron starts to fire (spiking threshold) remains roughly the same.

Figure 5 shows that as predicted by the Leaky Integrate-and-Fire (LIF) model, there is a noticeable increase in the rate as the resting battery approaches the neuronal threshold. This relationship is represented by both models showing a progressive increase in firing rate with the rise in resting battery from -100 mV towards 20 mV This visualization underscores the influence of resting battery adjustments on neuronal excitability.

Figure 6 demonstrate a parallel increase in entropy with the same trend as the rate. As the resting battery approaches the threshold from -100 mV to 20 mV, the entropy rises, suggesting a consistent relationship with the increased firing rate. Higher entropy indicates greater unpredictability and richer complexity in the neuronal response. This ascent in entropy underscores the interdependence between rate and entropy, with the shaded areas around the plotted lines representing the standard error from the mean, providing a statistical measure of dispersion for the observed entropy values.

Contrary to the unnormalized entropy, normalized entropy inversely indicates the regularity of neuronal discharge. Figure 7 reveals that as the resting battery varies from -100 mV to 20 mV, the normalized entropy demonstrates a concave shape, suggesting a non-linear relationship with the resting battery and implying a nuanced interplay between regularity and complexity in the neuronal response. While both models exhibit this concave trend, the model without NMDA receptor influence shows a slight decline in regularity at the midpoint, raising questions about the influence of NMDA receptor activation on the predictability of neuronal firing.

Analyzing the mutual information of different neurons with the same output amidst varied complexities unveils critical insights into the underpinnings of neuronal complexity. The

various figures elucidate the nuanced dynamics arising from changes in resting battery and the roles they play in influencing neuronal communication, complexity, and selectivity.

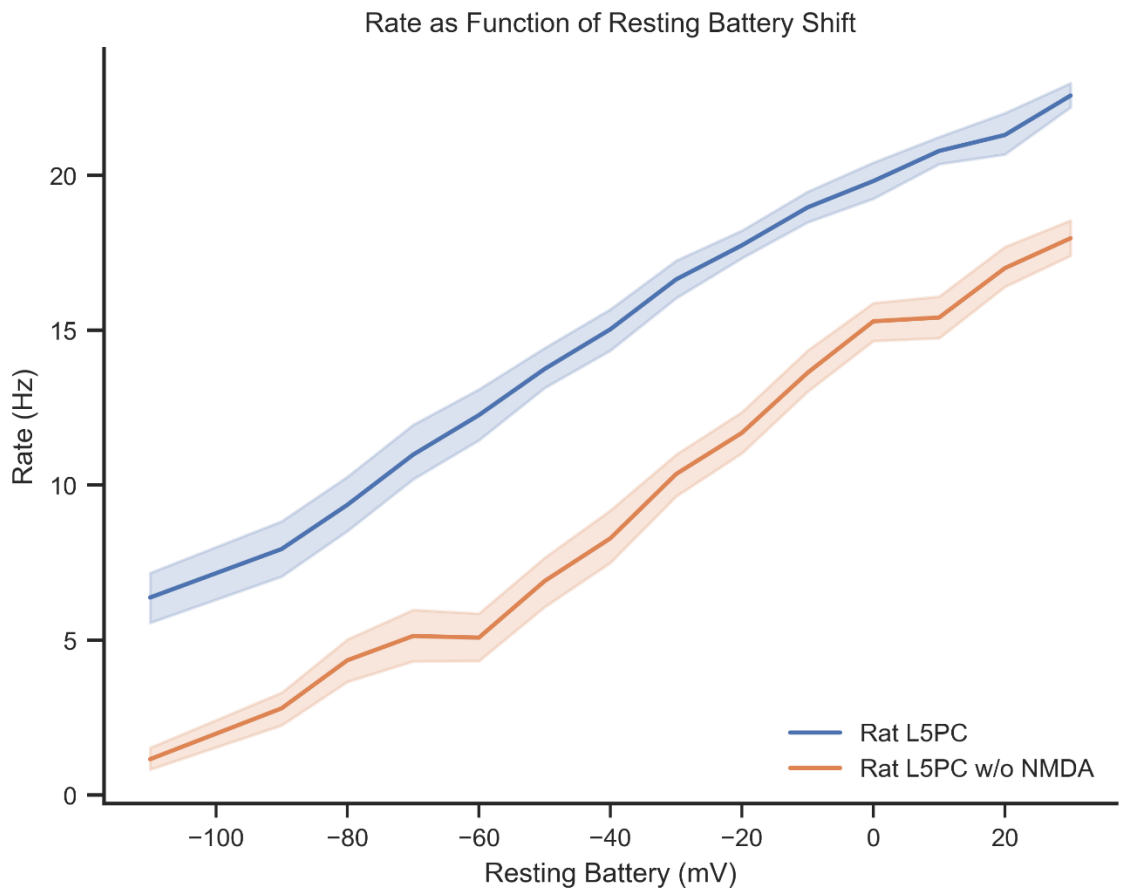

Figure 5. Rate Modulation as a Function of Resting Battery Level in Rat L5 Pyramidal Cells. Blue curve: the case where the resting battery change is due to NMDA receptor activity. Orange: the case where the NMDA receptors replace by AMPA only channels (Rat L5PC w/o NMDA). . The shaded area represents the 95% confidence interval, indicating where we expect the true mean values to lie with a high level of certainty.

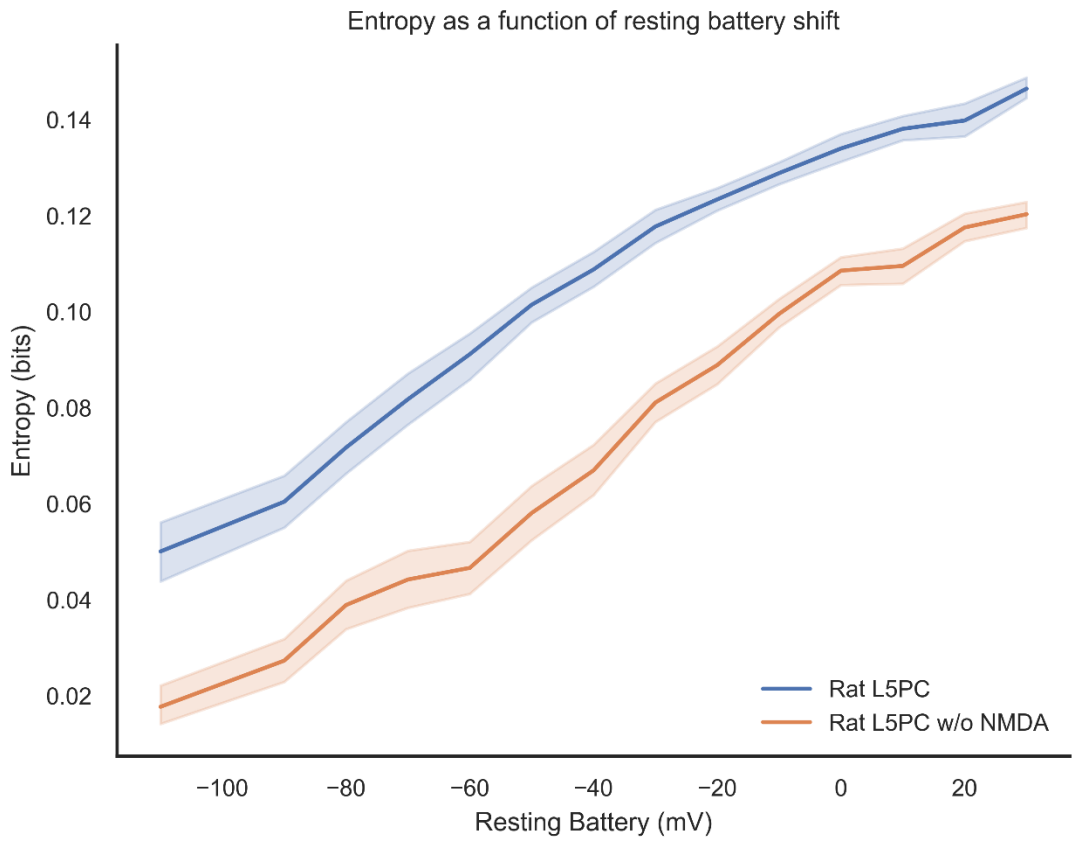

Figure 6. Entropy Variation with Resting Battery in Rat L5 Pyramidal Cells. The figure depicts the dynamic change in entropy as a function of the resting battery in Rat Layer 5 Pyramidal Cells (L5PC), under two conditions: with active NMDA receptors (Rat L5PC) and without NMDA receptor activation (Rat L5PC w/o NMDA). The shaded area represents the 95% confidence interval, indicating where we expect the true mean values to lie with a high level of certainty.

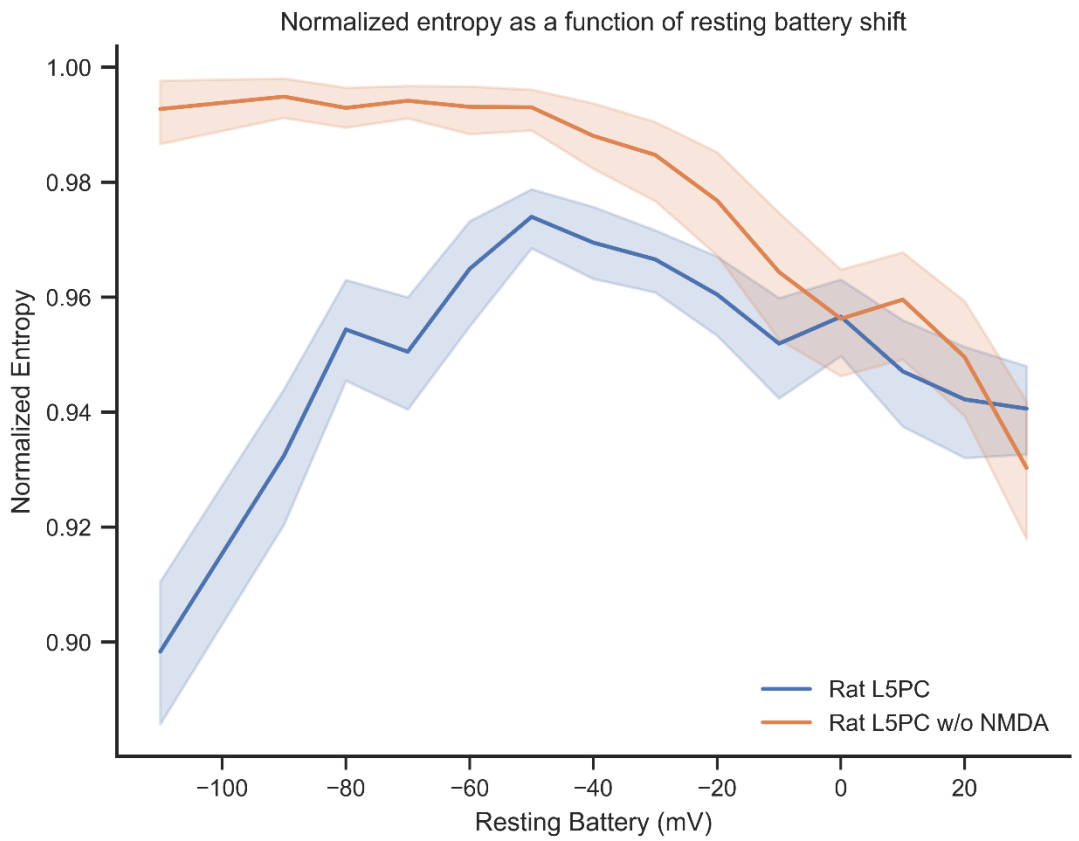

Figure 7. Regularity of Response Reflected in Normalized Entropy Across Resting Battery Variations. The figure delineates the trend in normalized entropy as a function of resting battery changes in Rat Layer 5 Pyramidal Cells, under the same two conditions: with active NMDA receptors (Rat L5PC) and without (Rat L5PC w/o NMDA). The shaded area represents the 95% confidence interval, indicating where we expect the true mean values to lie with a high level of certainty.

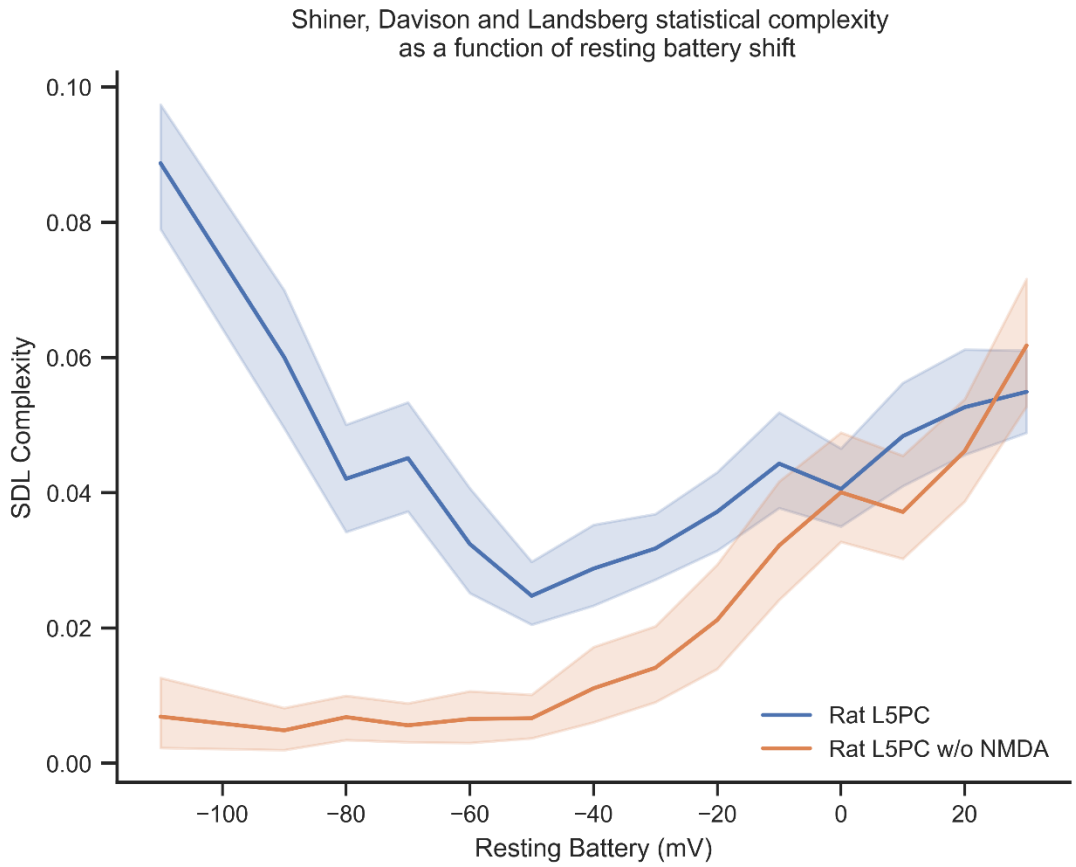

Figure 8. Shiner, Davison, and Landsberg Statistical Complexity as a Function of Resting Battery Change. The figure visualizes the Shiner, Davison, and Landsberg (SDL) statistical complexity in relation to changes in the *resting battery* for Rat Layer 5 Pyramidal Cells. It compares two scenarios: one with active NMDA receptors (Rat L5PC) and the other without (Rat L5PC w/o NMDA). The shaded area represents the 95% confidence interval, indicating where we expect the true mean values to lie with a high level of certainty.

Integrating Insights for Neuronal Complexity

The detailed comparison of the Rat L5bPC model with and without NMDA synapses, subject to identical inputs but varied passive channel equilibria, casts light on the intricate relationship between resting battery shifts and neuronal complexity. The increment in firing rate and entropy (echoes the heightened information content and complexity) as shown in Figure 6. However, the nuanced variations, especially in normalized entropy, unfold a deeper narrative of order, chaos, and the delicate equilibrium therein (Figure 7).

The unveiling of convergence in SDL complexity as resting battery shift accentuates underscores the intricate amalgamation of order and randomness that defines the essence of neuronal communication.

Figure 8 shows that as the resting battery increases from -100 mV to 20 mV, we observe a convex trend indicating that SDL complexity initially decreases and then increases, suggesting a non-monotonic relationship between resting battery and complexity. Both models exhibit convergence in complexity with increasing resting battery, indicating that the presence of NMDA receptors might be less influential at higher resting battery levels. This convergence pattern prompts an exploration into how shifts in resting battery influence the intricate balance between order and randomness in neuronal activities, and how the modulation of NMDA channels may impact on this complex dynamic.

The analyses in Figure 8 provide important insights, leading us into the complex world of neurons. The oscillation between order and chaos, the intricate dance of entropy and rate, and the subtle nuances unveiled by SDL complexity (all converge to sculpt a rich, multidimensional landscape). This unveils unprecedented avenues for understanding neuronal complexities. Each figure, in its eloquent narrative, contributes to demystifying the enigmatic dance of order and chaos that defines the core of neuronal interactions and complexities.

Increasing Synaptic Conductance and Comparison of Various Models

We further investigate different models: Rat L5bPC with and without NMDA synapses (which in turn will be replaced by AMPA only synapses) And Human L23 cell by Eyal at al [22] one with Rat L23 morphology and one with the original human morphology. We took the method even further and increased the inhibitory and excitatory synapses conductance by a factor, resulting in enhancing and decreasing the effect of single synapses on the spike output (see Methods for the actual conductance).

In this phase of the investigation, insights garnered from the observed variations in entropy (Figure 9, Figure 10) and SDL statistical complexity among the four different models: Rat L5bPC with and without NMDA synapses, and Human L23 cell by Eyal et al., both in its original and Rat L23 morphological configurations. These models were subjected to modifications in synaptic conductance to explore their responsive characteristics and inherent complexities.

Across all models, as maximal conductance increases, there is a concomitant rise in entropy, as seen in Figure 9, indicating a more unpredictable and complex neural activity pattern.

The trend lines for each model exhibit a positive correlation between conductance and entropy. This observation aligns with the general understanding that greater synaptic input, represented by conductance, can increase the complexity of a neuron's output. However, as inferred from Figure 13 and the correlation matrix in Figure 16, entropy's relationship with maximal conductance does not fully capture the underlying dynamics, suggesting that additional factors contribute to the observed neuronal behavior.

Figure 10 shows a notable divergence in the response of the Human L23 model, which experiences a sharp decline in normalized entropy as conductance increases. This suggests a unique adaptability and functional diversity in the Human L23 cells compared to the other models. The changing slope for Human L23 Indicates a more significant change in regularity or predictability of response with increasing synaptic input. Conversely, the Rat L5PC AMPA only model show a more subtle variation in normalized entropy, reflecting lower different complexities and response patterns, possibly because the lack of non-linearity comparing to the other models which has NMDA channels.

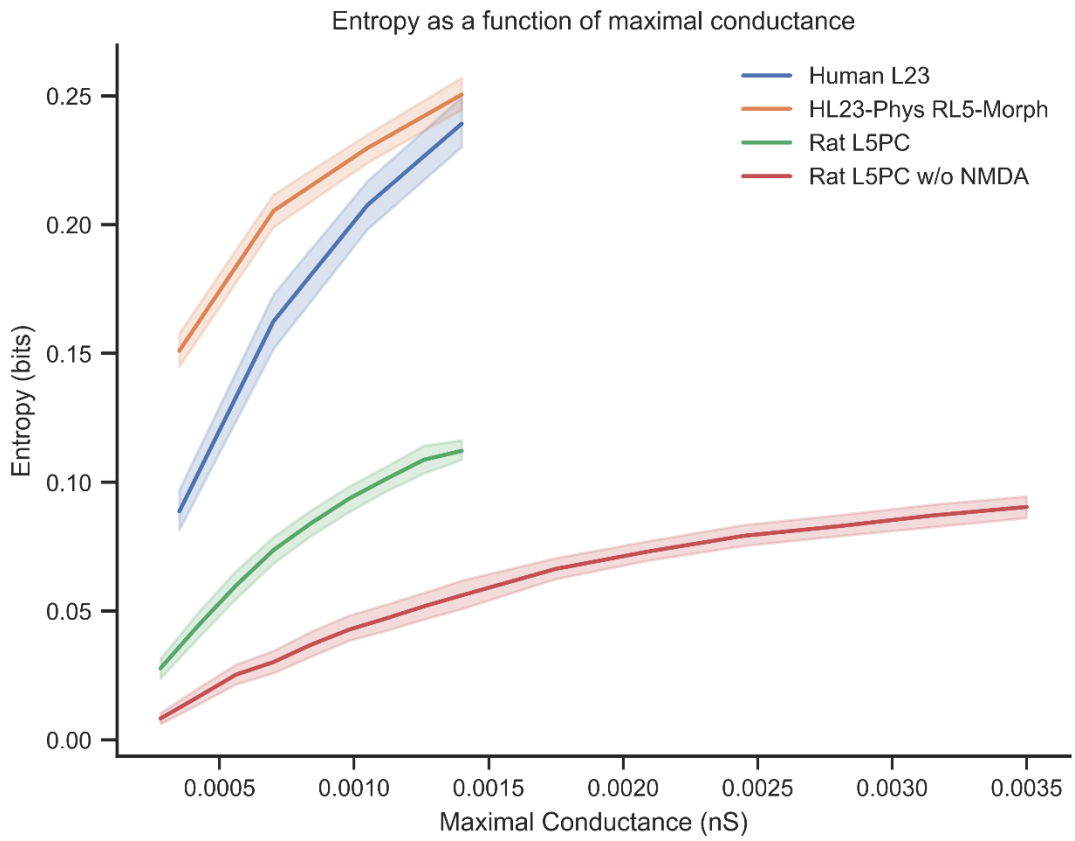

Figure 9. Entropy Trends in Relation to Maximal Synaptic Conductance Across Different Models. Here we explore the relationship between entropy and maximal synaptic conductance (measured in nano siemens) in various neuronal models. Included are human Layer 2/3 models—the Human L23 and a hybrid model combining Human L23 physiology with Rat Layer 5 morphology—and Rat Layer 5 Pyramidal Cell models, both with (Rat L5PC) and without NMDA receptors (Rat L5PC w/o NMDA). The shaded area represents the 95% confidence interval, indicating where we expect the true mean values to lie with a high level of certainty.

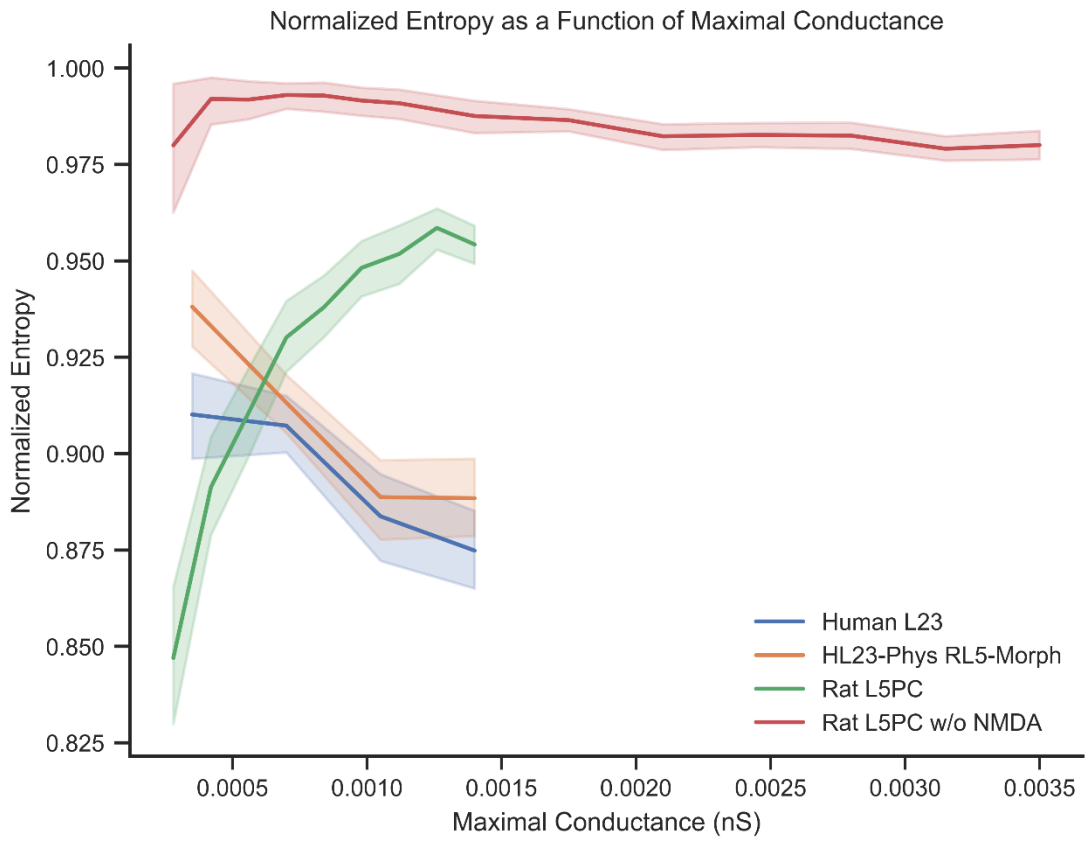

Figure 10. Variations in Normalized Entropy with Maximal Synaptic Conductance in Neuronal Models. *P*resents the variations in normalized entropy across a range of maximal synaptic conductance values for different neuronal models, including human Layer 2/3 models—the Human L23 and a hybrid model combining Human L23 physiology with Rat Layer 5 morphology—and Rat Layer 5 Pyramidal Cell models, both with (Rat L5PC) and without NMDA receptors (Rat L5PC w/o NMDA). The shaded area represents the 95% confidence interval, indicating where we expect the true mean values to lie with a high level of certainty.

Figure 11 and Figure 18 shifts focus to SDL statistical complexity, presenting a clear alignment with the pre-established complexity hierarchy of the models. The Human L23PC emerges as the most complex entity, followed sequentially by the Human L23PC with Rat morphology, Rat L5PC, and finally, the Rat L5PC without NMDA. The differences in complexity are highlighted by changes in synaptic conductance, which also prove the expected levels of complexity.

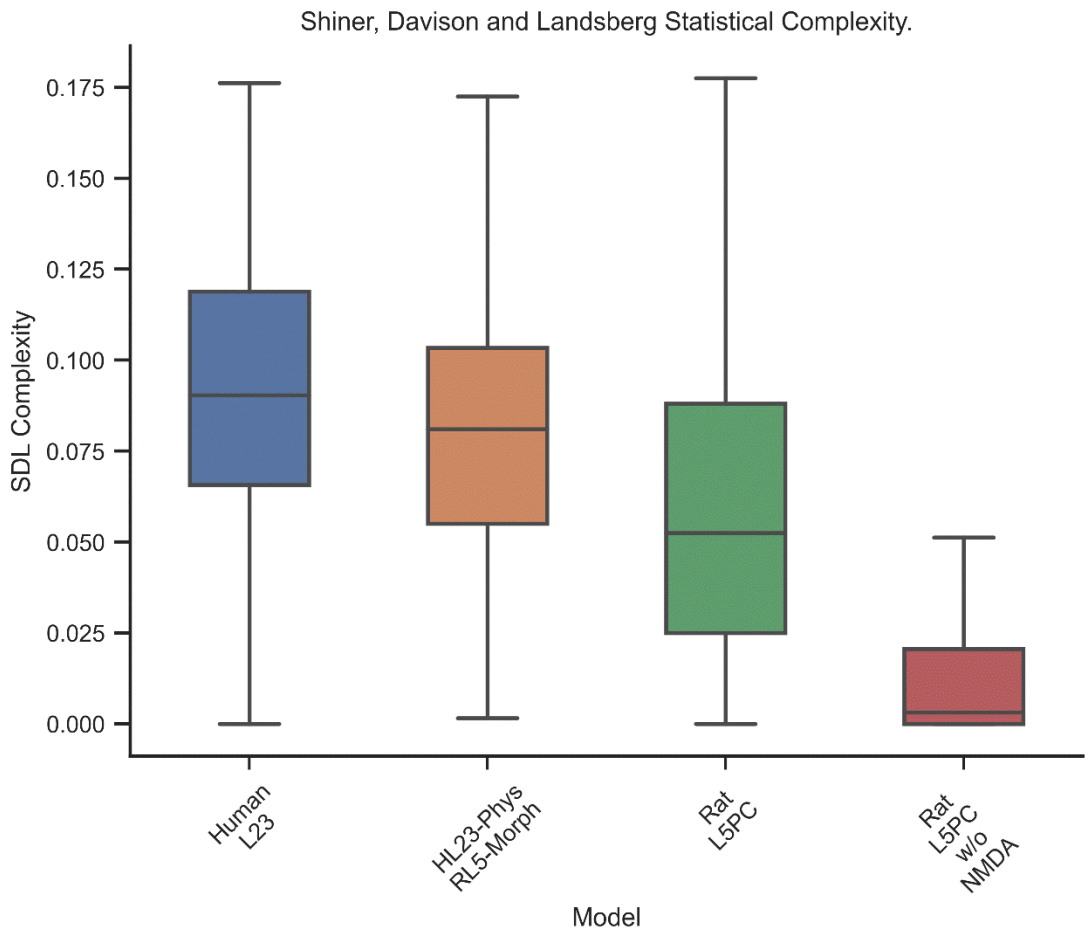

Figure 11. SDL Statistical Complexity Across Different Neuronal Models. provides a box plot analysis of the Shiner, Davison, and Landsberg (SDL) statistical complexity for four neuronal models. The models compared are human Layer 2/3 models—the Human L23 and a hybrid model combining Human L23 physiology with Rat Layer 5 morphology—and Rat Layer 5 Pyramidal Cell models, both with (Rat L5PC) and without NMDA receptors (Rat L5PC w/o NMDA). The complexity levels are clearly differentiated among the models, with the Human L23 showing the highest complexity, as indicated by the median and interquartile range, and the Rat L5PC w/o NMDA showing the lowest. The box plots illustrate the spread and variability of complexity within each model, with the tails of the plots indicating the range.

The amplified synaptic conductance delineated distinct behavioral patterns among the models. Each model's response underscored its inherent architectural and functional attributes, painting a diversified landscape of neuronal complexity. Figure 10 illustrates significant differences between human L23PC and rat L5PC models in terms of function. The Human L23PC, marked by heightened entropy and a rapid decline in normalized entropy, embodies an intricate array of structural and dynamic functional elements. In contrast, the Rat L5PC models,

though reflective of moderate complexities, encapsulate an essential blend of functional diversity and constraints.

These observations collectively weave an intricate narrative of the dynamic and nuanced landscape of neuronal complexities. The modulations induced by variations in synaptic conductance illuminate the distinct architectural, functional, and dynamic attributes of each model, offering a rich tapestry of insights into the multifaceted world of neuronal dynamics and complexities.

Methods

Presynaptic Input Data

As described by Beniaguev , Segev, and London (2021) [15], we employed Poisson processes in our study to produce presynaptic spike trains featuring smoothed piecewise constant instantaneous firing rates. The Gaussian smoothing sigma and the constant rate duration before smoothing were independently resampled for each 60-second simulation, with the initial 500 milliseconds being omitted and values ranging from 10 milliseconds to 600 milliseconds. Furthermore, the study incorporated the probability of synchronization, deactivation, and specific synaptic clustering. This methodology, as opposed to using a constant firing rate, sought to increase the temporal variation in the data, thereby bolstering the significance and generalizability of the results to a wide range of situations. Each recording of the 80 recording that had been done was for 60,500 milliseconds.

Postsynaptic Models

Models were based on the Rat L5bPC [16] and the Human L23PC [22] with $g_{max} = 0.0007$ for all the AMPA/NMDA/GABAA synapses in rat model and with $g_{max} = 0.0007$ for the GABAA synapses and $g_{max} = 0.00073027$ for the AMPA/NMDA synapses in human model. Each recording of the 80 recordings that had been done, was for 1 minute, the entropy was computed on the resolution of 1 millisecond (60,000 length sequence).

Training and Comparing ANN

In our methodology, we constructed a temporal convolutional neural network for each neuron, following the guidelines laid out in references [15] and [23] .These networks were applied to identical input patterns but were distinct in their output models: one tailored for the L5PC model (as per [16]) and the other for its reduced version [17], with both starting from the same initial weights. The training of these networks was conducted layer-wise (layers 1, 3, 5, and 7), focusing on achieving convergence in the loss function.

For the evaluation phase, we employed the Area Under the Curve (AUC) metric. This AUC metric, pivotal in machine learning, assesses the performance of classification models by calculating the area under the Receiver Operating Characteristic (ROC) curve, represented by the formula:

$$AUC = \int_0^1 TPR(FPR)d(FPR) \tag{1}$$

The ROC curve plots the true positive rate (TPR) against the false positive rate (FPR) across different thresholds. In this context, a higher AUC score, which can range from 0 to 1, correlates with higher model performance. A score of 1.0 signifies perfect classification, while 0.5 indicates no discriminative power.

Mutual Information Estimation

Shannon's mutual information between random variables X,Y is:

$$\max\big(H(X), H(Y)\big) \geq I(X;Y) = H(Y) - H(Y|X) \geq 0 \tag{2}$$

In the case of noiseless channel, we get.

$$H(Y|X) = 0 \rightarrow I(X;Y) = H(Y) \tag{3}$$

The mutual information metric quantifies the amount of information shared between two variables, X and Y. Specifically, it measures the reduction in uncertainty about one variable given knowledge of the other, expressed in terms of the number of bits needed on average to describe the information transmitted from X to Y. This metric is essential for understanding the extent to which the knowledge of one variable reduces uncertainty about the other.

Entropy Estimation

Approximating the entropy of binary time series ,specifically time series was done previously by Gao, Kontoyiannis and Bienenstock [24] Infinite Context Tree Weighted(CTW) as described in [25] [26] was used in order to calculate the entropy of each spike trains.

Normalized Entropy

We can notice one constraint on the postsynaptic output and that is that the neuron outputs are single dimension while his input is multidimensional therefore it will be bound from above by the maximum entropy of a single dimension process which is the entropy of the uniform distribution over all possible states.

We then can calculate the normalized entropy over a given spike trains with length of T and time resolution of Δt denoted by

$$s_m \in \left\{ s | s \in \{0,1\}^{\frac{T}{\Delta t}} \wedge |s| = m \right\} \tag{4}$$

(which is a vector of binned time of length $\frac{T}{\Delta t}$ with m spikes in it)

The uniform probability for each state is

$$P(\omega) = \frac{1}{\binom{\frac{T}{\Delta t}}{m}} \frac{m!\left(\frac{T}{\Delta t}-m\right)!}{\frac{T}{\Delta t}!} \tag{5}$$

and the entropy:

$$H_{max}(S_m) = \ln\left(\frac{\frac{T}{\Delta t}}{m!\left(\frac{T}{\Delta t}-m\right)!} \right) \tag{6}$$

The normalized entropy will be then:

$$\widehat{H}(S_m) = \frac{H(S_m)}{H_{max}(S_m)} \tag{7}$$

With the bound

$$0 \leq \widehat{H}(S_m) \leq 1 \tag{8}$$

Now we have a measure of the postsynaptic neuron output that is invariant to the firing rate.

SDL Complexity

SDL complexity is mentioned at [21][27] where the simplest form is:

$$SDL(X) = \frac{H(X)}{H_{max}(X)} \cdot \left(1 - \frac{H(X)}{H_{max}(X)}\right) \tag{9}$$

Comparisons

Comparisons between models were made by using the same presynaptic input patterns and analyzing their results.

Resting Battery Comparisons

To evaluate two models, the one with the NMDA was normalized by scaling the original model's maximal conductance by a factor of 0.2 to compare the models with the same rate. The passive equilibria were adjusted to different values to attain the desired resting battery shift.

Conductance Factor Comparisons

To assess the change in the conductance factor, we applied various maximal conductance scaling factors to the different models ranges as shown in the results.

Discussion

Rigidity and fluidity

What distinguishes neurons with low mutual information from those with high mutual information? Our hypothesis posits that the key difference lies in the balance between memory stability and learning rate. In the case of a neuron characterized by low mutual information (and thus rigidity), the limited amount of information it processes leads to smaller changes in synaptic plasticity (e.g., reduced calcium influx). Conversely, when a neuron exhibits high mutual information, it processes a more diverse range of information, which is not specific to any pattern. As a result, this "fluid" neuron undergoes fewer orderly updates in its synaptic weights, leading to a higher learning rate and decreased memory stability.

Regarding Hebbian plasticity, the idea that varied mutual information might dictate adaptation and consolidation is an extrapolation from Hebb's postulate itself. Some parts of the circuit continuously adapting might ensure robustness against noise while others are consolidating and stabilizing information.

The importance of the functional parts of a circuit

Balancing Roles of Neurons Circuits in the brain are intricate networks where different neurons contribute to a wide range of processing tasks. The differential mutual information across neurons suggests a balance between processing tasks and maintaining stability in representations. Neurons with low mutual information may be akin to those involved in maintaining stable, long-term knowledge. For example, certain neural populations have been observed to exhibit consistent firing patterns in response to persistent stimuli, indicating a form of stability in their representations such as spontaneous noise or oscillatory patterns in the cortex.

On the flip side, neurons with high mutual information might be more responsive to diverse stimuli, reminiscent of the concept of adaptive neurons. Some neurons, especially in the early sensory areas, show greater adaptability in response to novel stimuli [28] [7]. The high mutual information in these neurons represents how well they encode incoming stimuli, aiding in their adaptability. Their higher learning rates suggest they play roles in periods of rapid learning [29].

This diversity in neural operations, facilitated by varying levels of mutual information, forms the crux for complex computations, including those involving learning, memory, and adaptation.

In Conclusion This discussion underscores the likely roles of neurons with varied mutual information levels. Such a division may be an evolutionary adaptation, offering both adaptability and consistency in information processing. The adaptive neurons, with higher mutual information, are pivotal during periods of rapid learning and adaptability to novel stimuli, while those with lower mutual information contribute to maintaining stable representations, thereby ensuring a balanced and efficient functioning of neural circuits.

Potential of Mutual Information Measurements in Circuit Analysis

The intricate workings of neural circuits have long been a subject of intense study, with numerous methods employed to probe their mysteries. The measure of mutual information offers a promising avenue in this quest. By comparing the mutual information of different neurons with the same presynaptic input, we can potentially glean insights into the functional roles and responsiveness of individual neurons within a circuit. Such a comparison would not only help distinguish between neurons that are more adaptable versus those that prioritize stability but also shed light on the mechanisms underpinning these differences.

This comparative approach could revolutionize our understanding of neural circuits. It promises to unravel the unique contributions of individual neurons to overall circuit function. By harnessing the insights gained from these analyses, we might be better positioned to comprehend the complexities of neural computations, from basic sensory processing to advanced cognitive tasks. This enhanced understanding could bridge gaps in our current knowledge, guiding future research directions and refining our brain function models.

Assessing mutual information in vivo

Measuring mutual information in vivo on sustained stimuli provides a method to analyze individual neuron responsiveness within neural circuits. By examining mutual information on a per-neuron basis, insights into the functional roles and adaptability versus stability of neurons can be gleaned. This approach could help identify “complex” neurons with high mutual

information, indicative of greater adaptability to diverse stimuli, and contrast them with neurons exhibiting lower mutual information, which may represent stability in information processing. Through such analyses, a more nuanced understanding of neural circuits and their role in complex computations could be achieved, aiding in the broader exploration of brain function.

Conclusions

Our research has presented a novel approach to delineate the functionality of neurons by assessing the volume of information relayed from presynaptic to postsynaptic neurons. Leveraging the concept of mutual information, we have been able to delve deeper into the computational proficiencies of individual neurons. This offers valuable insights into their probable contributions in determining the varied behaviors we observe in natural settings.

Furthermore, this method empowers us to ascertain the distinctive functionalities of cells based on a specific distribution. It aids in quantifying the bits of information that traverse through the collective ensemble of presynaptic neurons to their postsynaptic counterparts. Our comparisons across multiple models substantiated the hypothesis that NMDA synapses amplify the intricacy of neurons. Conversely, fortifying the synapses diminishes this complexity, primarily as each synapse regulates the neuron’s voltage, rendering it increasingly vulnerable to noise. This observation was consistently mirrored in the resting battery shift models, further validating our proposed framework.

To deepen our understanding, evaluating various models devoid of internal noise and subjected to identical inputs might present a promising avenue. This could elucidate the influence of diverse inputs on the plethora of models at our disposal.

Supplementary Figures

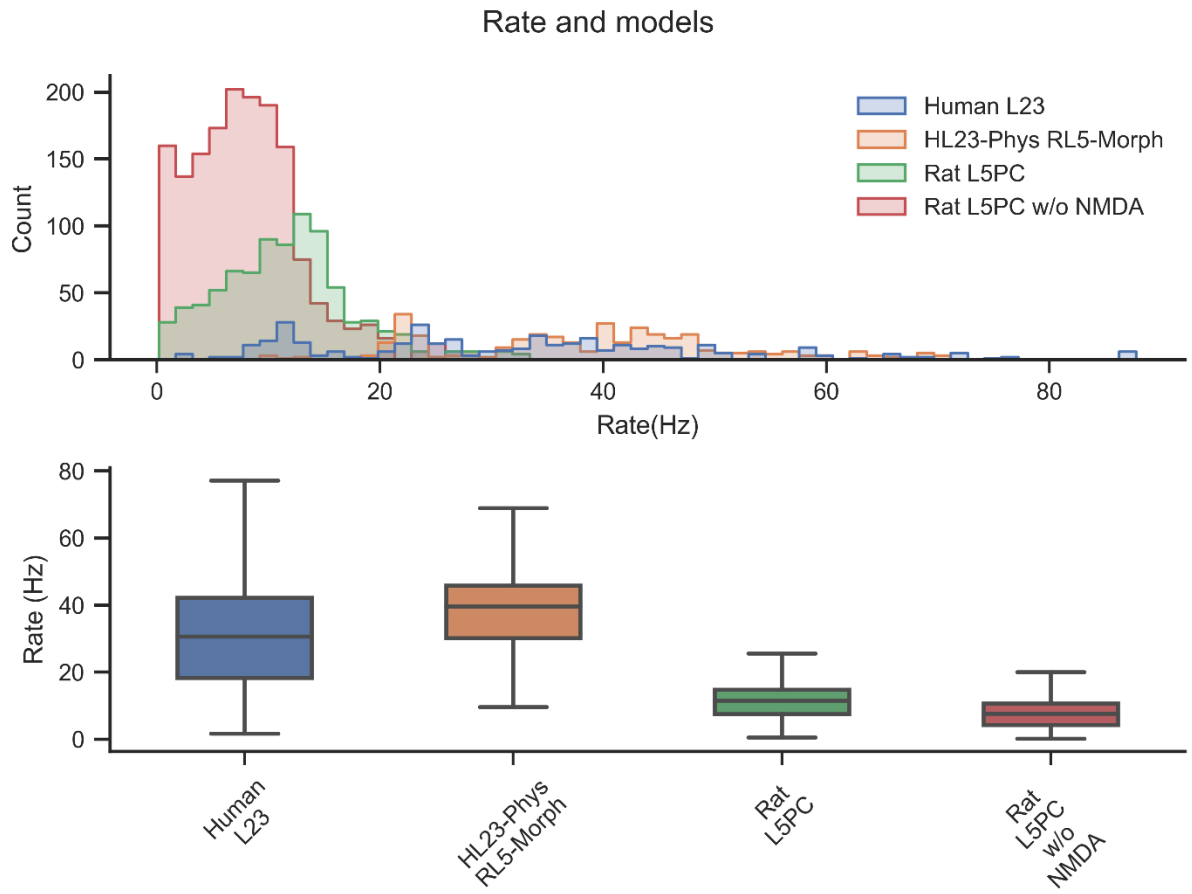

Figure 12. Rate Distributions and Variability Across Neuronal Models. The figure illustrates the distribution and variability of firing rates across a selection of neuronal models. The top histogram details the occurrence frequency of different rate values for Human L23, Human L23 physiology with rat morphology, and Rat L5PC, both with and without NMDA resting battery influence. Each model's rate distribution is color-coded, allowing for an assessment of overlap and dispersion. The bottom box plot provides a statistical summary of the same rate data, highlighting the median, quartiles, and outliers, thus offering a clear comparison of central tendency and variability among the models. This combined graphical representation serves to elucidate the comparative dynamics of neuronal firing rates, as influenced by morphological and physiological variations.

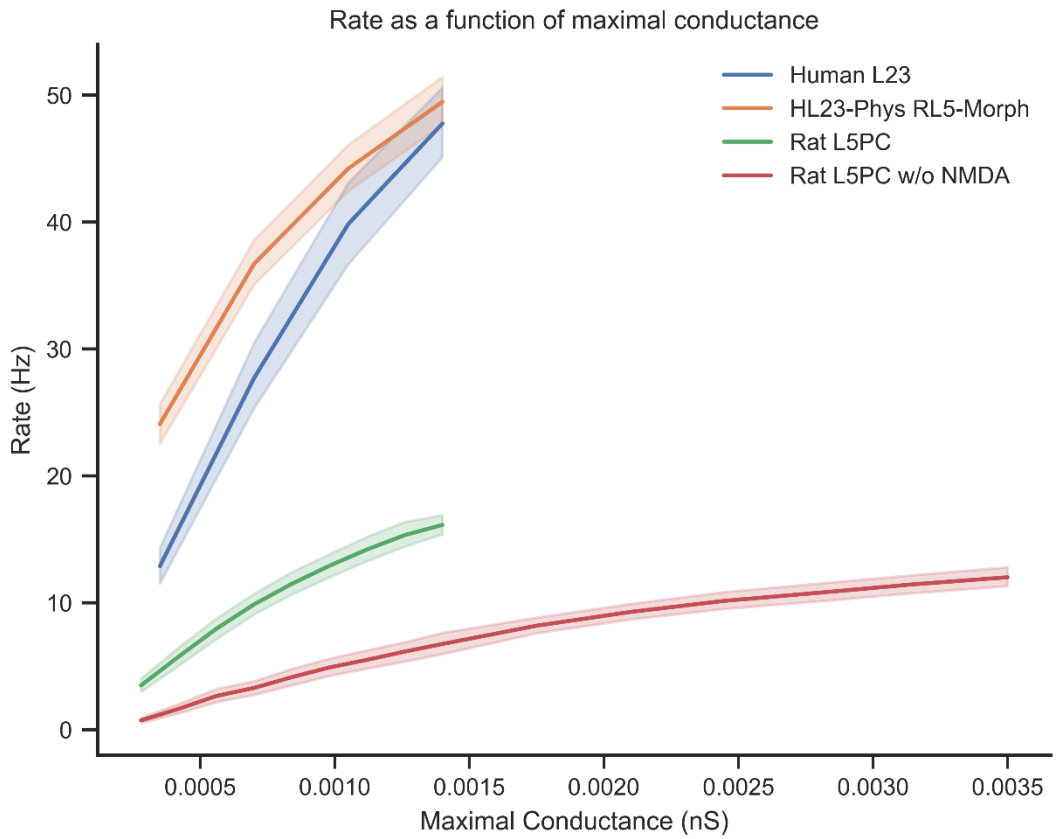

Figure 13. Firing Rate Responses to Maximal Synaptic Conductance in Neuronal Models. The figure displays the relationship between firing rates and maximal synaptic conductance for four different neuronal models: Human L23, Human L23 rat morph, Rat L5PC, and Rat L5PC without NMDA receptors. The graph shows a clear trend where increases in maximal conductance correspond to higher rates for each model. The Human L23 and its rat morphological counterpart exhibit similar patterns of increase, with the human model showing slightly higher rates at corresponding conductance levels. The Rat L5PC model demonstrates a less steep relationship, indicating a different sensitivity to conductance changes compared to human models. Notably, the Rat L5PC without NMDA receptors shows the lowest rate response across the conductance range, suggesting that NMDA receptor activity significantly contributes to the firing rate. The shaded regions around each line denote the standard error, reflecting the variability in the measurement. The shaded area represents the 95% confidence interval, indicating where we expect the true mean values to lie with a high level of certainty.

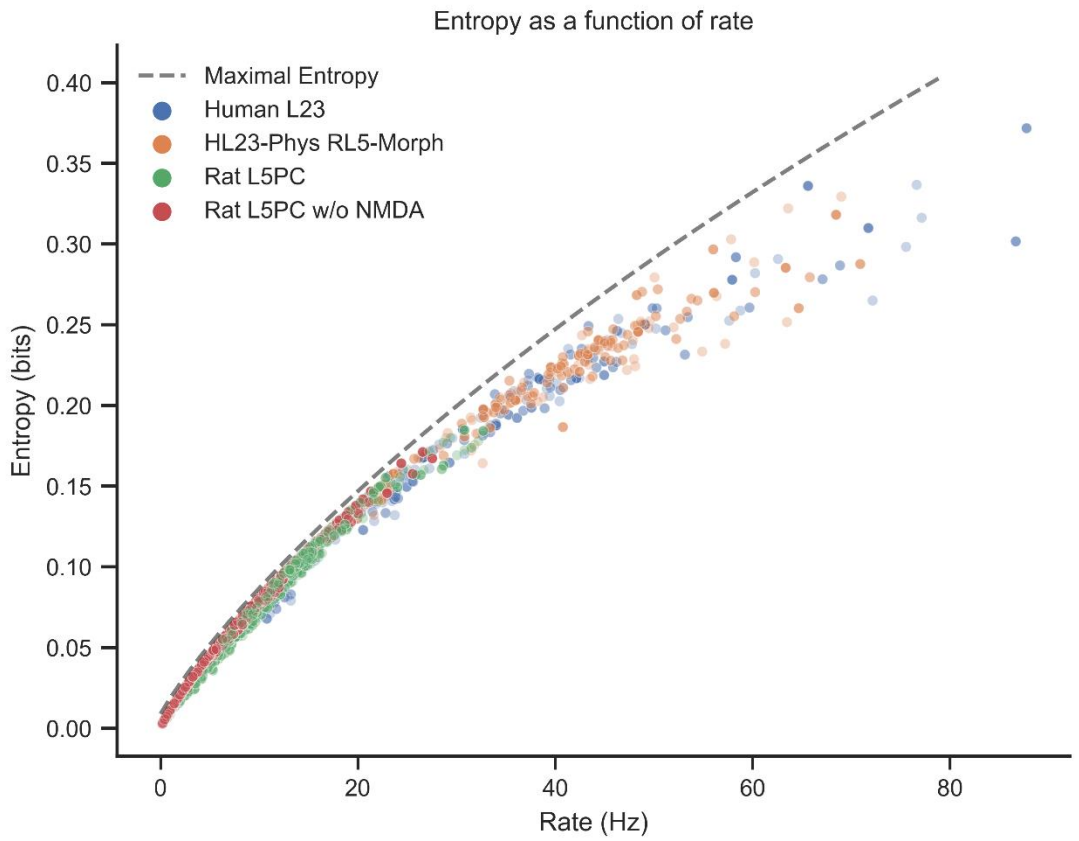

Figure 14. Entropy Dependency on Firing Rate in Various Neuronal Models. The figure portrays the correlation between entropy and firing rate for a set of neuronal models: Human L23, Human L23 with rat morphological alterations, Rat L5PC, and Rat L5PC without NMDA receptors. The scatter plot aggregates data points from multiple instances, with each model represented by a unique color. A dashed line indicating 'Maximal Entropy' suggests a theoretical or observed upper limit of entropy across rates. The data points collectively exhibit a positive correlation; as the firing rate increases, there is a corresponding rise in entropy, implying more variability in the firing patterns at higher rates. This trend holds true across all models, though with varying degrees of slope, which may reflect differences in the complexity or adaptability of each model's firing patterns. The spread of data points around the line of maximal entropy highlights the range within which each model operates under the given experimental conditions.

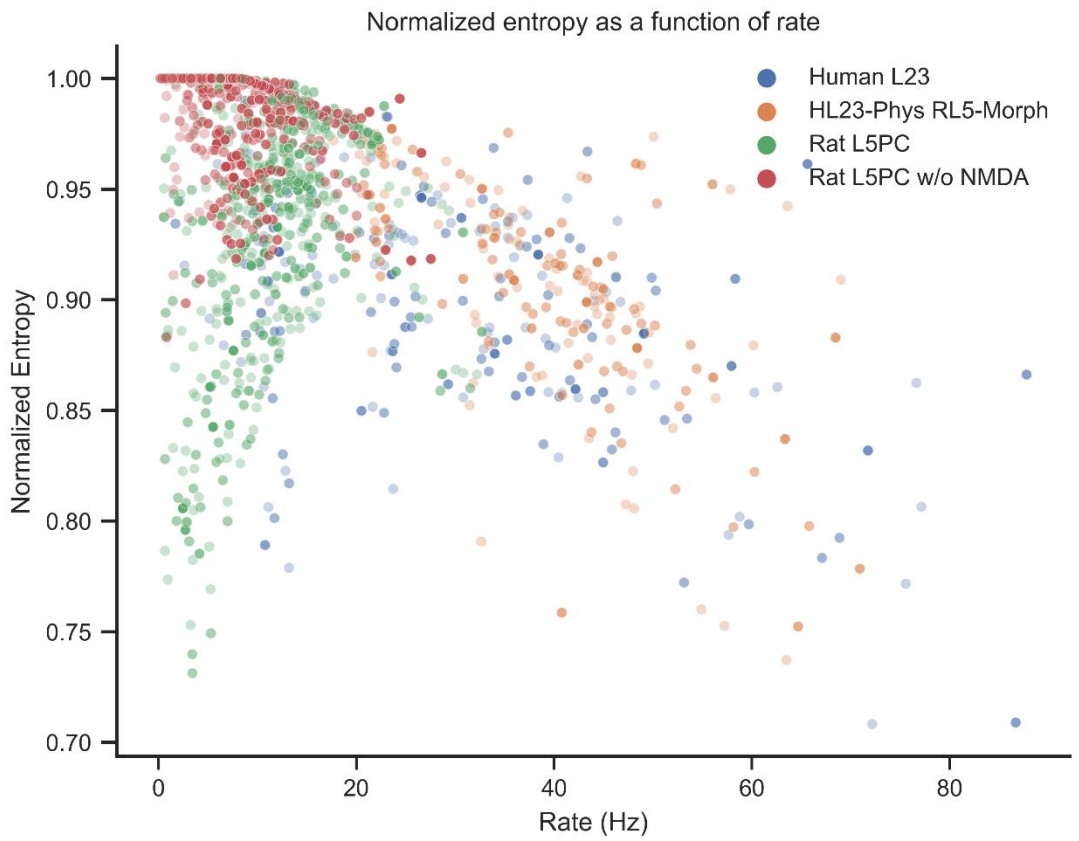

Figure 15. Correlation of Normalized Entropy with Firing Rate in Neuronal Models. The figure displays the relationship between normalized entropy and firing rate for a collection of neuronal models, including Human L23, Human L23 physiology with rat morphological adjustments, Rat L5PC, and Rat L5PC without the influence of NMDA receptors. Each model is represented by a distinct color in the scatter plot, which shows the entropy normalization for a range of firing rates. The plot suggests a general trend where higher firing rates correspond to lower normalized entropy, particularly noticeable in the Human L23 model. This inverse relationship indicates that as neurons fire more rapidly, the predictability of their firing patterns increases, thus reducing normalized entropy. The Rat L5PC models, especially without NMDA receptors, display a broader distribution of normalized entropy across rates, pointing to different intrinsic dynamics in entropy modulation compared to human models. The dense clustering of data points at lower rates reveals the models' behavioral consistency at baseline firing levels.

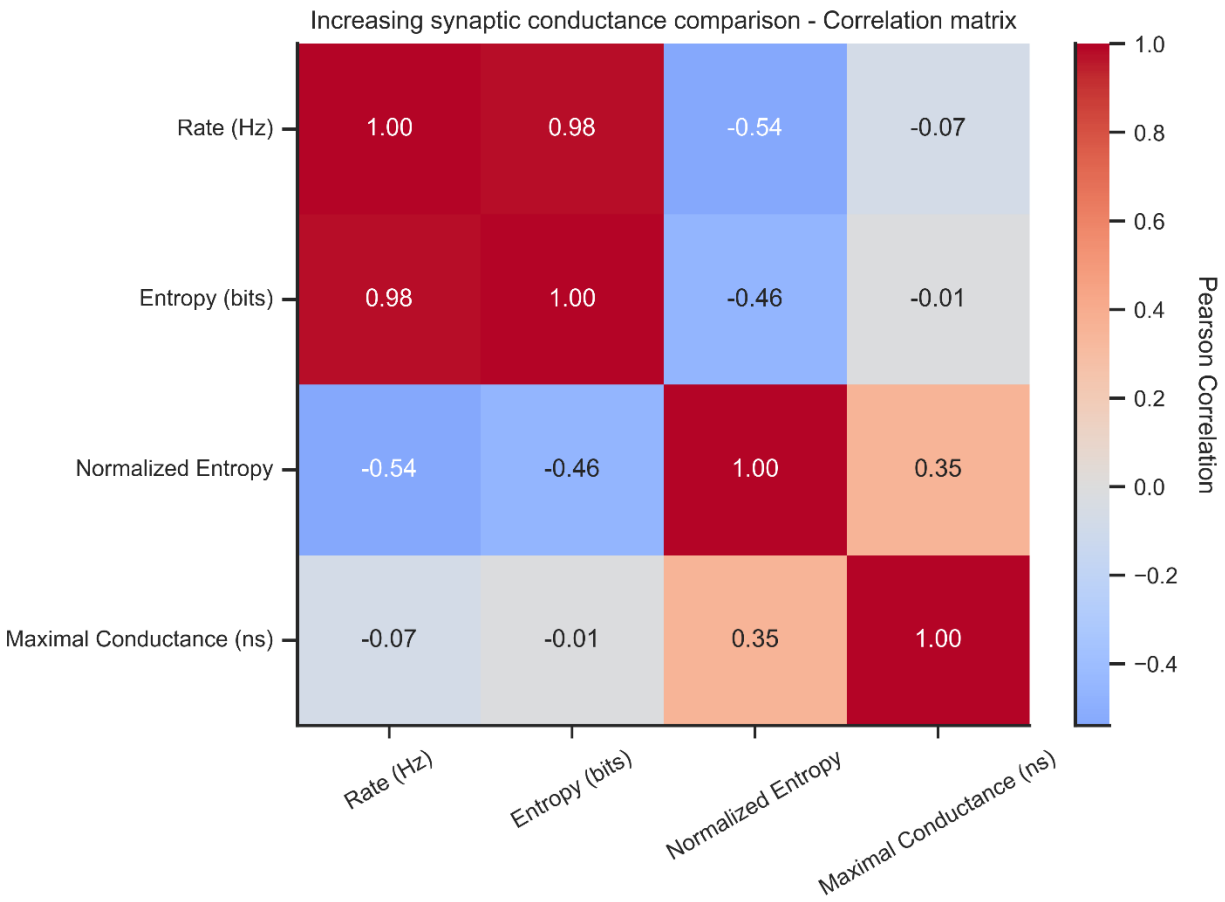

Figure 16. Correlation Matrix of Neuronal Properties with Increasing Synaptic Conductance. The correlation matrix quantitatively describes the relationships between various neuronal properties such as rate, entropy, normalized entropy, and maximal synaptic conductance (measured in nano siemens). The matrix provides correlation coefficients ranging from -1 to 1, where 1 indicates a perfect positive correlation, -1 indicates a perfect negative correlation, and 0 indicates no correlation. According to the matrix, rate and entropy show a very high positive correlation (0.98), suggesting they increase together. Normalized entropy has a moderate positive correlation (0.36) with maximal conductance, which is the strongest correlation involving maximal conductance, indicating that as the conductance increases, there is a tendency for normalized entropy to increase as well. In contrast, rate and normalized entropy display a negative correlation (-0.43), implying that as the firing rate increases, the normalized entropy tends to decrease. The color gradient from blue to red visually emphasizes the strength and direction of these correlations.

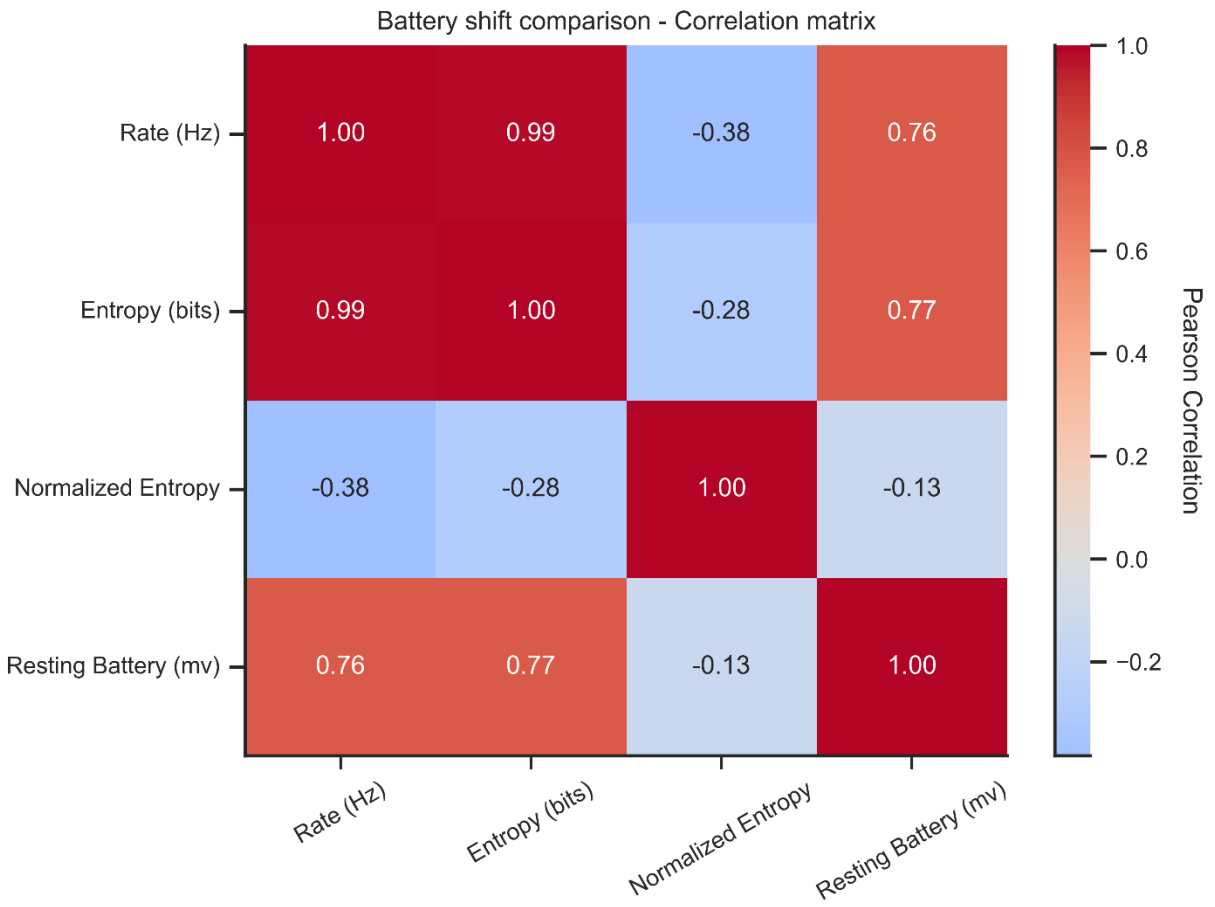

Figure 17. Resting Battery Shift is Correlated Highly with Rate and Entropy. The correlation matrix quantitatively describes the relationships between various neuronal properties such as rate, entropy, normalized entropy, and maximal synaptic conductance (measured in nano siemens). The matrix provides correlation coefficients ranging from -1 to 1, where 1 indicates a perfect positive correlation, -1 indicates a perfect negative correlation, and 0 indicates no correlation. According to the matrix, rate and entropy show a very high positive correlation (0.98), suggesting they increase together. Normalized entropy has a moderate positive correlation (0.36) with maximal conductance, which is the strongest correlation involving maximal conductance, indicating that as the conductance increases, there is a tendency for normalized entropy to increase as well. In contrast, rate and normalized entropy display a negative correlation (-0.43), implying that as the firing rate increases, the normalized entropy tends to decrease. The color gradient from blue to red visually emphasizes the strength and direction of these correlations.

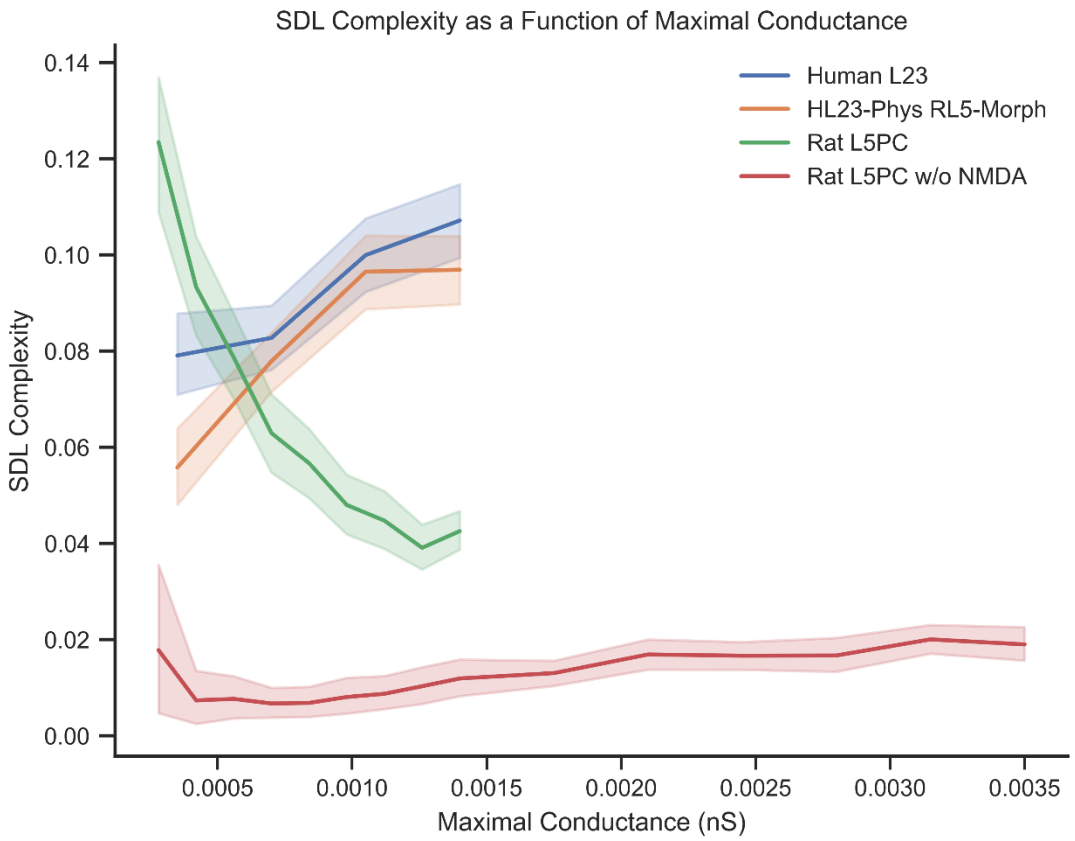

Figure 18 SDL Complexity as A Function of Maximal Conductance. The figure displays the relationship between The SDL statistical complexity and maximal synaptic conductance. The models compared are human Layer 2/3 models—the Human L23 and a hybrid model combining Human L23 physiology with Rat Layer 5 morphology—and Rat Layer 5 Pyramidal Cell models, both with (Rat L5PC) and without NMDA receptors (Rat L5PC w/o NMDA). The complexity levels are clearly differentiated among the models except the point where there is intersection with g_{max}= 0.0006 , with the Human L23 showing the highest complexity, and the Rat L5PC w/o NMDA showing the lowest across all of the maximal conductance values. The shaded area represents the 95% confidence interval, indicating where we expect the true mean values to lie with a high level of certainty.

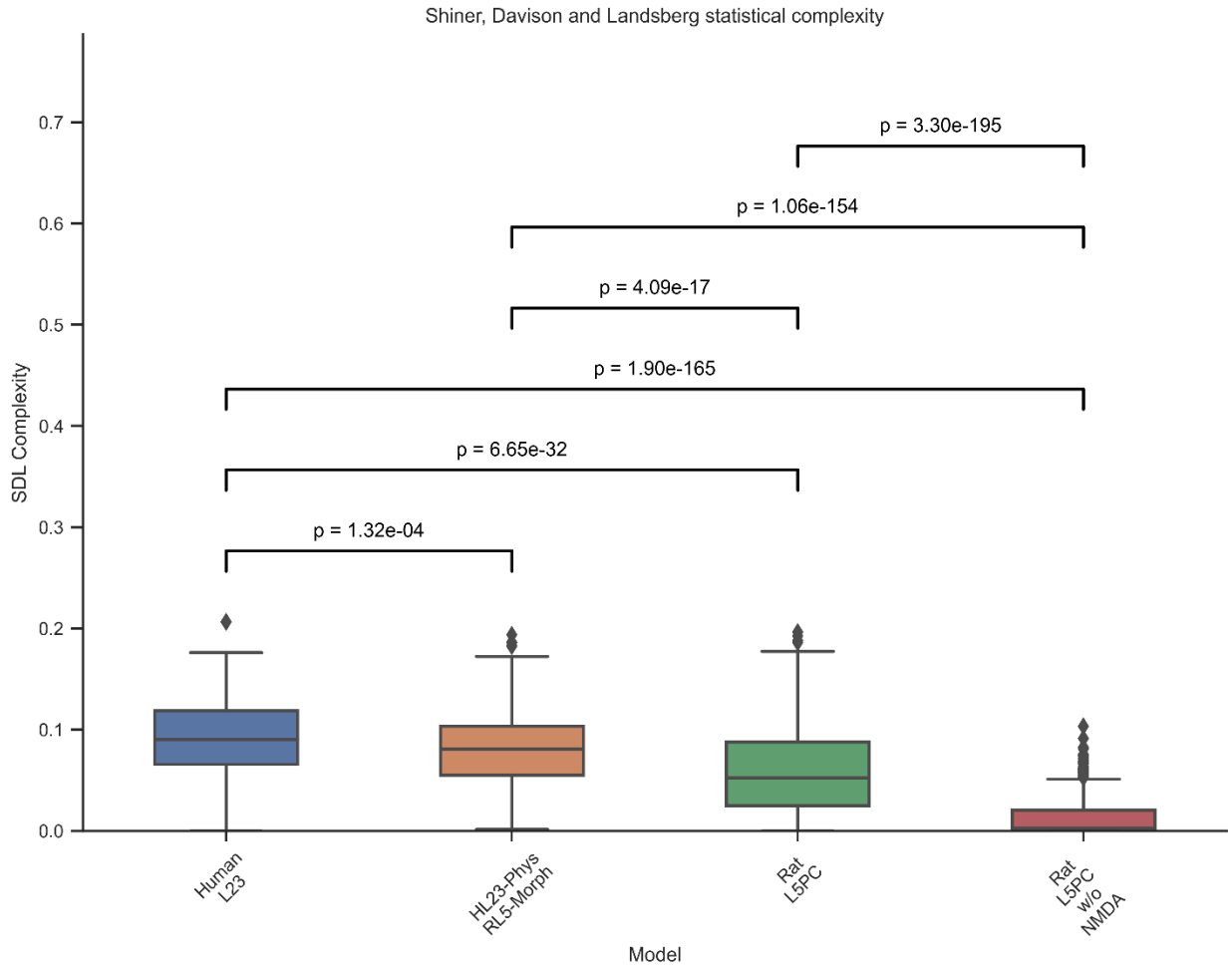

Figure 19. SDL Complexity and Statistical Significance Across Neuronal Models. The box plot illustrates the SDL complexity for different neuronal models—Human L23, Human L23 physiology with rat morphology, Rat L5PC, and Rat L5PC without NMDA receptors—alongside the statistical significance (p-values) of differences between them. The box plots show the median, interquartile range, and outliers for each model's complexity. Overlaid on the plot are brackets indicating pairwise comparisons between models with corresponding p-values, which denote the statistical significance of the difference in complexities. The extremely low p-values (ranging from 1.32e-04 to 1.46e-175) confirm that the differences in complexity between the models are highly significant. Notably, the Rat L5PC without NMDA receptors shows a markedly lower complexity compared to the other models, as evidenced by its lower median and smaller interquartile range. These p-values provide a robust quantification of the disparities observed, supporting the hypothesis that morphological and synaptic properties significantly influence the computational complexity of neuronal models.

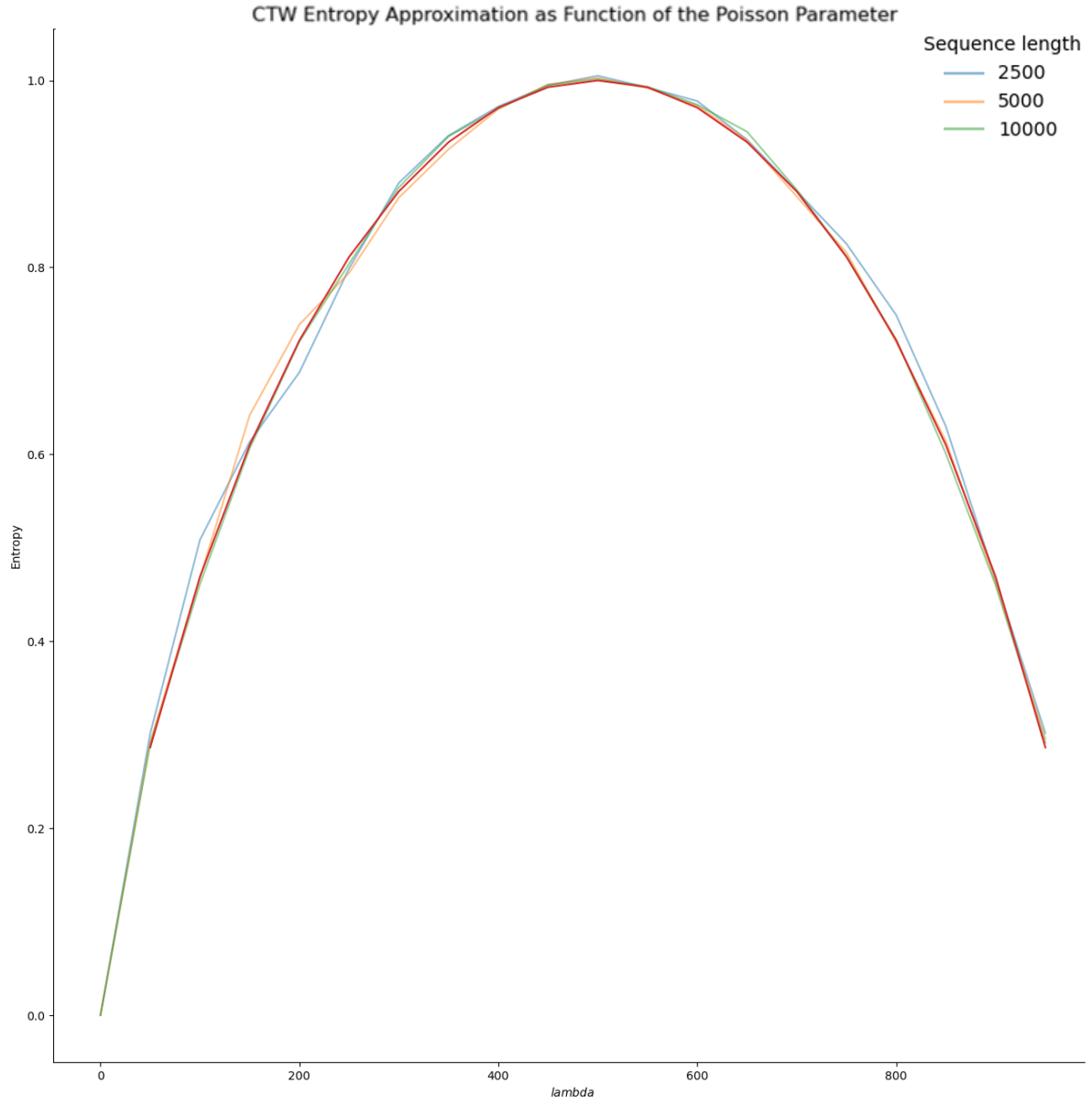

Figure 20. Validation of CTW Algorithm on Poisson Random Variable. As a sanity check we evaluate the Context Tree Weighting (CTW) algorithm's performance in estimating the entropy of a Poisson random variable at different rates of occurrence (λ). The x-axis denotes the lambda parameter scaled by 1/1000, while the y-axis represents the entropy estimated by the CTW algorithm. Three curves correspond to sequence lengths of 2500, 5000, and 10000, each indicating the entropy approximation's consistency across sequence lengths (analytical solution in red). The graph shows that the CTW algorithm's entropy estimations align closely for all sequence lengths, particularly at intermediate λ values, where the entropy reaches a peak before declining. This pattern validates the CTW algorithm's effectiveness in capturing the intrinsic randomness of the Poisson process, with the peak entropy reflecting the point of maximum uncertainty or variability in the distribution.

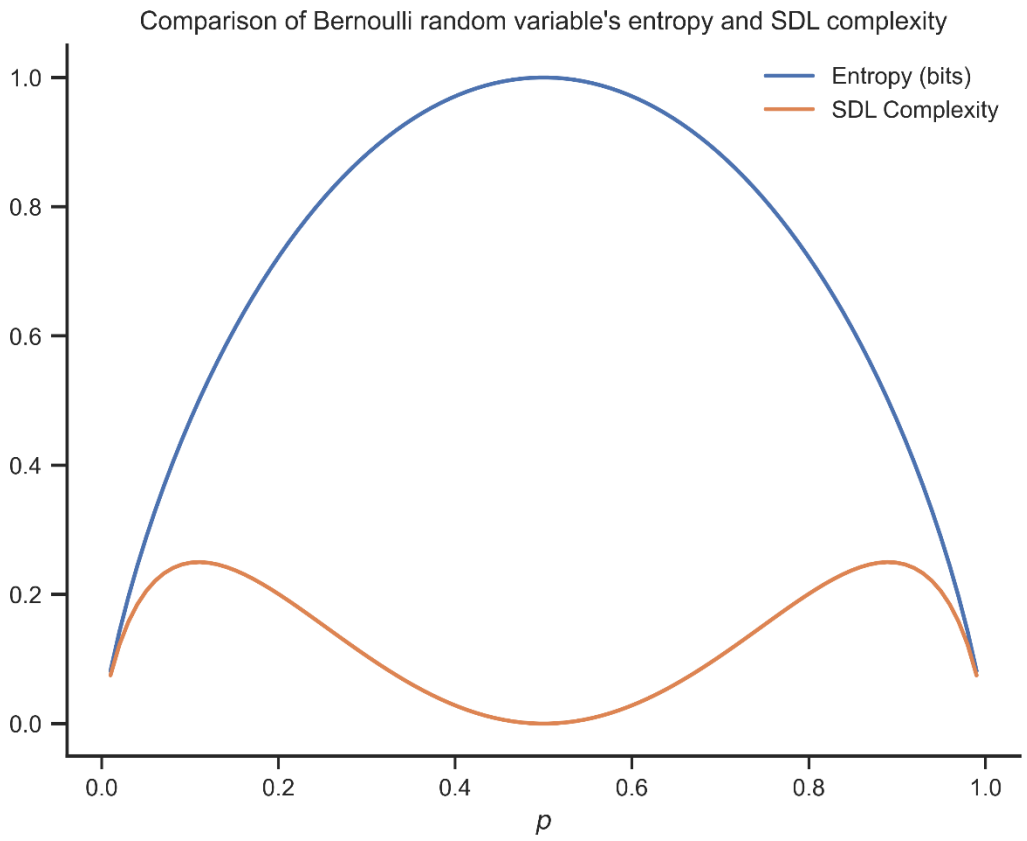

Figure 21. Intuitive Visualization of Entropy and SDL Complexity for a Bernoulli Random Variable. The figure presents a comparative analysis of entropy and SDL complexity for a Bernoulli random variable across different probabilities of success (p). The x-axis represents p, ranging from 0 to 1, while the y-axis quantifies both entropy and SDL complexity, accommodating their respective scales. Two distinct curves, each representing one of the two metrics, are plotted. The entropy curve is undefined at $p = 0$ and $p = 1$, indicating zero entropy in these deterministic scenarios. It ascends to reach a peak at $p = 0.5$,where the uncertainty is maximized due to the equal likelihood of success and failure, and then symmetrically descends as p approaches 1. In contrast, the SDL complexity curve, while also undefined at $p = 0$ and $p = 1$, exhibits a different pattern. It rises to a peak near $p = 0.11$ and $p = 0.89$ and then declines to reach its lowest point at $p = 0.5$, rising again symmetrically towards $p = 1$. This illustrates that the SDL complexity is not highest when the uncertainty is maximized.

Reference

[1] N. Perez-Nieves, V. C. H. Leung, P. L. Dragotti and D. F. M. Goodman, "Neural heterogeneity promotes robust learning," *Nature Communications,* vol. 12, October 2021.

[2] M. London and M. Häusser, "DENDRITIC COMPUTATION," *Annual Review of Neuroscience,* vol. 28, p. 503–532, July 2005.

[3] M. London, A. Schreibman, M. Häusser, M. E. Larkum and I. Segev, "The information efficacy of a synapse," *Nature Neuroscience,* vol. 5, p. 332–340, March 2002.

[4] F. Grammont and A. Riehle, "Spike synchronization and firing rate in a population of motor cortical neurons in relation to movement direction and reaction time," *Biological Cybernetics,* vol. 88, p. 360–373, May 2003.

[5] T. Brosch and H. Neumann, "Interaction of feedforward and feedback streams in visual cortex in a firing-rate model of columnar computations," *Neural Networks,* vol. 54, p. 11–16, June 2014.

[6] D. Ji and M. A. Wilson, "Firing Rate Dynamics in the Hippocampus Induced by Trajectory Learning," *The Journal of Neuroscience,* vol. 28, p. 4679–4689, April 2008.

[7] S. G. Solomon and A. Kohn, "Moving Sensory Adaptation beyond Suppressive Effects in Single Neurons," *Current Biology,* vol. 24, p. R1012–R1022, October 2014.

[8] H. S. Orer, M. Das, S. M. Barman and G. L. Gebber, "Fractal Activity Generated Independently by Medullary Sympathetic Premotor and Preganglionic Sympathetic Neurons," *Journal of Neurophysiology,* vol. 90, p. 47–54, July 2003.

[9] A. S. Charles, M. Park, J. P. Weller, G. D. Horwitz and J. W. Pillow, "Dethroning the Fano Factor: a flexible, model-based approach to partitioning neural variability," July 2017.

[10] C. E. Shannon, "A Mathematical Theory of Communication," *Bell System Technical Journal,* vol. 27, p. 379–423, July 1948.

[11] F. Rosenblatt, "The perceptron: A probabilistic model for information storage and organization in the brain.," *Psychological Review,* vol. 65, p. 386–408, 1958.

[12] P. Poirazi, T. Brannon and B. W. Mel, "Pyramidal Neuron as Two-Layer Neural Network," *Neuron,* vol. 37, p. 989–999, March 2003.

[13] T. Moldwin and I. Segev, "Perceptron Learning and Classification in a Modeled Cortical Pyramidal Cell," *Frontiers in Computational Neuroscience,* vol. 14, April 2020.

[14] B. A. Bicknell and M. Häusser, "A synaptic learning rule for exploiting nonlinear dendritic computation," *Neuron,* vol. 109, p. 4001–4017.e10, December 2021.

[15] D. Beniaguev, I. Segev and M. London, "Single cortical neurons as deep artificial neural networks," *Neuron,* vol. 109, p. 2727–2739.e3, September 2021.

[16] E. Hay, S. Hill, F. Schürmann, H. Markram and I. Segev, "Models of Neocortical Layer 5b Pyramidal Cells Capturing a Wide Range of Dendritic and Perisomatic Active Properties," *PLoS Computational Biology,* vol. 7, p. e1002107, July 2011.

[17] O. Amsalem, G. Eyal, N. Rogozinski, M. Gevaert, P. Kumbhar, F. Schürmann and I. Segev, "An efficient analytical reduction of detailed nonlinear neuron models," *Nature Communications,* vol. 11, January 2020.

[18] M. Megias, Z. Emri, T. F. Freund and A. I. Gulyas, "Total number and distribution of inhibitory and excitatory synapses on hippocampal CA1 pyramidal cells," *Neuroscience,* vol. 102, p. 527–540, February 2001.

[19] P. Channell, I. Fuwape, A. B. Neiman and A. L. Shilnikov, "Variability of bursting patterns in a neuron model in the presence of noise," *Journal of Computational Neuroscience,* vol. 27, p. 527–542, June 2009.

[20] R. López-Ruiz, H. L. Mancini and X. Calbet, "A statistical measure of complexity," *Physics Letters A,* vol. 209, p. 321–326, December 1995.

[21] J. S. Shiner, M. Davison and P. T. Landsberg, "Simple measure for complexity," *Physical Review E,* vol. 59, p. 1459–1464, February 1999.

[22] G. Eyal, M. B. Verhoog, G. Testa-Silva, Y. Deitcher, R. Benavides-Piccione, J. DeFelipe, C. P. J. de Kock, H. D. Mansvelder and I. Segev, "Human Cortical Pyramidal Neurons: From Spines to Spikes via Models," *Frontiers in Cellular Neuroscience,* vol. 12, June 2018.

[23] C. Lea, M. D. Flynn, R. Vidal, A. Reiter and G. D. Hager, *Temporal Convolutional Networks for Action Segmentation and Detection,* arXiv, 2016.

[24] Y. Gao, I. Kontoyiannis and E. Bienenstock, "Estimating the Entropy of Binary Time Series: Methodology, Some Theory and a Simulation Study," *Entropy,* vol. 10, p. 71–99, June 2008.

[25] F. M. J. Willems, Y. M. Shtarkov and T. J. Tjalkens, "The context-tree weighting method: basic properties," *IEEE Transactions on Information Theory,* vol. 41, p. 653–664, May 1995.

[26] F. M. J. Willems, "The context-tree weighting method: extensions," *IEEE Transactions on Information Theory,* vol. 44, p. 792–798, March 1998.

[27] M. T. Martin, A. Plastino and O. A. Rosso, "Generalized statistical complexity measures: Geometrical and analytical properties," *Physica A: Statistical Mechanics and its Applications,* vol. 369, p. 439–462, September 2006.

[28] J. Benda, "Neural adaptation," *Current Biology,* vol. 31, p. R110–R116, February 2021.

[29] T. O. Sharpee, A. J. Calhoun and S. H. Chalasani, "Information theory of adaptation in neurons, behavior, and mood," *Current Opinion in Neurobiology,* vol. 25, p. 47–53, April 2014.

[30] T. M. Cover and J. A. Thomas, Elements of Information Theory, Wiley, 2005.

[31] O. A. Rosso, H. A. Larrondo, M. T. Martin, A. Plastino and M. A. Fuentes, "Distinguishing Noise from Chaos," *Physical Review Letters,* vol. 99, p. 154102, October 2007.

[32] R. Stoop, N. Stoop, A. Kern and W.-H. Steeb, "Shiner–Davison–Landsberg complexity revisited," *Journal of Statistical Mechanics: Theory and Experiment,* vol. 2005, p. P11009–P11009, November 2005.

[33] P. V. Watkins and D. L. Barbour, "Rate-level responses in awake marmoset auditory cortex," *Hearing Research,* vol. 275, p. 30–42, May 2011.